C^2-continuous surface reconstruction with piecewise polynomial patches

Marc Wagner [a,1], Kai Hormann [b,2], Günther Greiner [a,3]

[a] *Friedrich-Alexander-Universität Erlangen-Nürnberg, Institut für Informatik 9, Am Weichselgarten 9, 91058 Erlangen, Germany*

[b] *California Institute of Technology, 1200 E California Boulevard, Pasadena, CA 91125, USA*

February 1, 2003

Abstract

In this report we describe a new method for generating a smooth surface that approximates a given manifold triangulation with arbitrary topology. At first we treat this problem in an axiomatic approach that does not depend on a specific surface type and derive a set of necessary conditions that guarantee the C^2-continuity of the result. Then we apply these conditions and develop an algorithm for generating a piecewise polynomial reconstruction surface that consists of a small number of patches. The method provides a set of intuitive parameters for shape control.

[1] mcwagner@immd9.informatik.uni-erlangen.de
[2] hormann@cs.caltech.edu
[3] greiner@informatik.uni-erlangen.de

1 INTRODUCTION

A common problem in the field of reverse engineering is to create a smooth surface that approximates a given manifold triangulation. The surface should be given in parametric form, in other words, as the image of a function $\mathbf{F} : D \to \mathbb{R}^3$ for some parameter domain $D \subset \mathbb{R}^2$. In order to handle objects with arbitrary topology, the reconstruction surface is usually represented as the collection of several surfaces $\mathbf{F}_i$ which we will also refer to as *surface patches* or simply *patches*.

This report presents a new method for generating a reconstruction surface from a given manifold triangulation with arbitrary topology. The reconstruction surface is C^2-continuous everywhere and consists of only a small number of patches. Each patch is either a low-order bivariate polynomial or a composition thereof and can therefore be stored and evaluated very efficiently. Furthermore, we introduce a set of control parameters that influence the shape of the reconstruction surface and have an obvious geometric meaning.

1.1 Previous work

Most of the existing methods that address the problem of constructing a smooth surface from a given triangulation can roughly be divided into two classes.

Methods of the first class decompose a given triangle mesh into a small number of segments, each of them containing many vertices. The segments are then reconstructed by individual surface patches, usually TP-B-spline-surfaces. The patches are then trimmed near the boundaries of the corresponding segments which results in gaps between neighbouring patches. The main effort now goes into filling these gaps with properly chosen blending surfaces. Most of these methods merely focus on generating C^1-continuous blends. Moreover, the blending surfaces and the trimmed patches usually do not meet exactly, but only within some user-specified precision. In other words, there are still gaps in the overall reconstruction surface but care is taken so as to make them smaller than, for example, the production tolerance. Examples of such methods are [FaSv96, HeKo96, KoMa00, VaBe98, VaHo98, VaRo97, WeRe99].

The second class of methods are those that decompose the triangle mesh into many segments, each of them containing a small number of vertices only. The segment boundaries are chosen in such a way that the shapes of the segments resemble the shapes of the parameter spaces of the surface patches (triangular shapes for Bézier-triangles, quadrangular shapes for TP-Bézier-surfaces or TP-B-spline-surfaces). The conditions that guarantee the continuity of the derivatives up to a certain order at the boundary of neighbouring surface patches are used as side constraints for the approximation process that fits each patch to the vertices of the corresponding segment. These methods do not require the surface patches to be trimmed and the overall reconstruction surface does not have any gaps. The main drawback of methods of this class is the large number of individual patches. Additionally, most of them yield C^1-continuous results only, e. g. [EcHo96, Loop94, WaMe96]. An exception is the work of Peters [Pete01] that guarantees C^2-continuity. But besides the large number of surface patches that are used to approximate the segments an even bigger number of additional blending surfaces is needed.

1.2 Overview

Our method belongs to the first class but we can guarantee the result to be C^2-continuous everywhere and without any gaps. The overall reconstruction process consists of the following steps.

We first decompose the given triangle mesh into several segments, each of them homeomorphic to a disc. For that purpose we developed an interactive tool that enables the user to partition even big triangle meshes in a short time. Then we parameterize and approximate each segment with a bicubic TP-B-spline-surface utilizing standard techniques. We describe these preprocessing steps briefly in Section 2.

We then define a set of appropriate trimming curves for each of the patches that were calculated during the preprocessing stage and generate several blending surfaces to connect these patches. We distinguish between *blending strips* that sew together those patches whose corresponding segments share a common boundary and *N-surface-blends* that are inserted whenever N segments meet at a common vertex. **The main contribution of this report is that we create the trimming curves as well as the blending surfaces such that the overall reconstruction surface is C^2-continuous everywhere.** We explain the basic idea of the method by means of two simple examples in Section 3. We then derive a set of necessary conditions that guarantee the C^2-continuity of the result in an axiomatic approach in Section 4. Sections 5 and 6 describe in detail how piecewise polynomial blending surfaces meeting these conditions can be constructed.

We close with a presentation of our results and a brief outlook to future work in Section 7.

1.3 Notations and conventions

Throughout this report we use the following notations and conventions.

1.3.1 Derivatives

Partial derivatives with respect to certain variables are denoted by using these variables as indices, e. g.,

$$\mathbf{F}_u(u,v) \equiv \frac{\partial}{\partial u}\mathbf{F}(u,v) \quad , \quad \mathbf{F}_{uu}(u,v) \equiv \frac{\partial^2}{\partial u^2}\mathbf{F}(u,v) \quad , \quad \mathbf{F}_{uv}(u,v) \equiv \frac{\partial}{\partial v}\frac{\partial}{\partial u}\mathbf{F}(u,v) \quad .$$

Partial directional derivatives with respect to certain directions are denoted by using the corresponding directions (usually unit vectors) as indices, e. g.,

$$\mathbf{F}_{\mathbf{e}}(u,v) \equiv \frac{\partial}{\partial \mathbf{e}}\mathbf{F}(u,v) = \langle \mathbf{grad}\,\mathbf{F}(u,v)\,,\,\mathbf{e}\rangle \quad .$$

1.3.2 The Kronecker delta

The Kronecker delta $\delta_{i,j}$ is defined by

$$\delta_{i,j} = \begin{cases} 1 & \text{if } i = j \\ 0 & \text{otherwise} \end{cases} \quad .$$

1.3.3 Parameter spaces

The parameter space of a function $\mathbf{F}$, introduced as $\mathbf{F}(u,v)$, is denoted by $D^{(u,v)}$. This is a very compact and practical notation because most of the functions that we define in the following sections share their parameter space with other functions. For example, it will be clear without stating it explicitly that $D^{(U,V)}$ is the parameter space of the functions $H^{\downarrow}(U,V)$, $H^{\uparrow}(U,V)$, $\mathbf{G}^{\downarrow}(U,V)$ and $\mathbf{G}^{\uparrow}(U,V)$ but not of $\mathbf{F}(u,v)$.

1.3.4 Polynomials

Although our method is not limited to polynomials in any way and can be applied to arbitrary functions, all functions used in this report are of polynomial type. We decided to use polynomials because they are commonly used to describe free form surfaces and supported by all CAD-systems.

There are three common representations of bivariate polynomial functions, namely TP-Bézier-surfaces, TP-B-spline-surfaces, and Bézier-triangles. Since all three are equivalent, i. e. conversion is possible without loss of information, we choose whatever representation is the most practical for a specific purpose.

A TP-Bézier-surface $\mathbf{F}(u,v)$ of degree (m,n) with a rectangular parameter space $D^{(u,v)} = [t_{u,0}, t_{u,1}] \times [t_{v,0}, t_{v,1}]$ is given by

$$\mathbf{F}(u,v) \;=\; \sum_{i=0}^{m}\sum_{j=0}^{n} B_i^{m,[t_{u,0},t_{u,1}]}(u)\, B_j^{n,[t_{v,0},t_{v,1}]}(v)\, \mathbf{b}_{i,j} \quad ,$$

where $\mathbf{b}_{i,j}$ are the control points and $B_\alpha^{\beta,[t_0,t_1]}$ are the Bernstein polynomials defined over the interval $[t_0,t_1]$,

$$B_\alpha^{\beta,[t_0,t_1]}(t) \;=\; \begin{pmatrix} \beta \\ \alpha \end{pmatrix} \left(\frac{t-t_0}{t_1-t_0}\right)^{\alpha} \left(1 - \frac{t-t_0}{t_1-t_0}\right)^{\beta-\alpha} \quad .$$

A TP-B-spline-surface $\mathbf{F}(u,v)$ of degree (m,n) with a rectangular parameter space $D^{(u,v)} = [t_{u,m}, t_{u,p}] \times [t_{v,n}, t_{v,q}]$ and knot vectors $\mathbf{U} = [t_{u,0}, \ldots, t_{u,m}, \ldots, t_{u,p}, \ldots, t_{u,p+m}]$ and $\mathbf{V} = [t_{v,0}, \ldots, t_{v,n}, \ldots, t_{v,q}, \ldots, t_{v,q+n}]$, is given by

$$\mathbf{F}(u,v) \;=\; \sum_{i=0}^{p-1}\sum_{j=0}^{q-1} N_i^{m,\mathbf{U}}(u)\, N_j^{n,\mathbf{V}}(v)\, \mathbf{d}_{i,j} \quad ,$$

where $\mathbf{d}_{i,j}$ are the control points and $N_\alpha^{\beta,\mathbf{T}}$ are the normalized B-spline-basis-functions,

$$N_\alpha^{0,\mathbf{T}}(t) \;=\; \begin{cases} 1 & \text{if } t \in [t_\alpha, t_{\alpha+1}) \\ 0 & \text{otherwise} \end{cases}$$

$$N_\alpha^{\beta,\mathbf{T}}(t) \;=\; \frac{t-t_\alpha}{t_{\alpha+\beta}-t_\alpha}\, N_\alpha^{\beta-1,\mathbf{T}}(t) \;+\; \frac{t_{\alpha+\beta+1}-t}{t_{\alpha+\beta+1}-t_{\alpha+1}}\, N_{\alpha+1}^{\beta-1,\mathbf{T}}(t) \quad , \quad \beta > 0 \quad .$$

A Bézier-triangle $\mathbf{F}(u,v)$ of degree m with a triangular parameter space $D^{(u,v)} = \Delta(\mathbf{R},\mathbf{S},\mathbf{T})$, $\mathbf{R} \in \mathbb{R}^2$, $\mathbf{S} \in \mathbb{R}^2$, $\mathbf{T} \in \mathbb{R}^2$ is given by

$$\mathbf{F}(u,v) \;=\; \sum_{i+j+k=m} B_{i,j,k}^{m}(u,v)\, \mathbf{b}_{i,j,k} \quad ,$$

where $\mathbf{b}_{i,j,k}$ are the control points and $B_{i,j,k}^m$ are the Bernstein polynomials defined over the triangle $\Delta(\mathbf{R},\mathbf{S},\mathbf{T})$,

$$B_{i,j,k}^{m}(u,v) \;=\; \begin{pmatrix} m \\ i \;\; j \;\; k \end{pmatrix} \rho(u,v)^i\, \sigma(u,v)^j\, \tau(u,v)^k \quad ,$$

where $\rho(u,v)$, $\sigma(u,v)$ and $\tau(u,v)$ are the barycentric coordinates of (u,v) relative to the corner points $\mathbf{R}$, $\mathbf{S}$ and $\mathbf{T}$ of the triangular parameter space.

Detailed informations about polynomial surfaces and their different representations can be found in [Schu81, BaBe87, Boor87, Fari97, HoLa93, Dier95].

2 PREPROCESSING

The preprocessing of our method consists of three sequential steps: segmenting the triangle mesh, parameterizing the segments and approximating each of the segments with a bicubic B-spline-surface.

2.1 Segmenting the triangle mesh

For the segmentation we developed an interactive tool that enables the user to decompose even big triangle meshes in a short time. The user specifies only a small number of vertices along the desired segment boundary by clicking at them with the mouse pointer. Two consecutively marked vertices are connected automatically with the shortest path along the edges of the triangulation. We define the length of a path $[\mathbf{r}_0, \mathbf{r}_1, \ldots, \mathbf{r}_n]$ as

$$\ell([\mathbf{r}_0, \mathbf{r}_1, \ldots, \mathbf{r}_n]) \quad = \quad \sum_{i=1}^{n} \|\mathbf{r}_{i-1} - \mathbf{r}_i\| \, \angle(\mathbf{r}_{i-1}, \mathbf{r}_i) \quad , \tag{1}$$

where $\angle(\mathbf{r}_{i-1}, \mathbf{r}_i)$ is the angle between the two triangles adjacent to the edge $(\mathbf{r}_{i-1}, \mathbf{r}_i)$. We find the shortest path with linear programming. The reason for multiplying the edge lengths with the angles is that paths along sharp creases are preferred this way. We found this strategy to give very natural segmentation boundaries. Figure 1 shows how a segment boundary was specified by three mouse clicks. Figure 2 shows examples of triangle meshes that were segmented with our tool.

2.2 Parameterizing the segments

Before approximating a segment $\mathcal{S}$ with a parametric surface $\mathbf{F}(u, v)$ we have to determine parameter values $\mathbf{p}_k = (u_k, v_k)$ for its vertices $\mathbf{r}_k$, $k = 1, \ldots, N$. A common way of doing this is to construct a continuous function $\psi : \mathcal{S} \to \mathbb{R}^2$ that is linear for each triangle in $\mathcal{S}$ and set $\mathbf{p}_k = \psi(\mathbf{r}_k)$ (see Figure 3). Such a parameterization ψ is of good quality if the distortion between $\mathcal{S}$ and $\psi(\mathcal{S})$ is small. There are many ways of measuring this distortion and finding ψ. We refer to [FlHo02] as a good survey. In our examples we have used a method proposed by Lévy et al. [LePe02] that is based on the concept of conformal mappings and determines ψ by solving a sparse linear system.

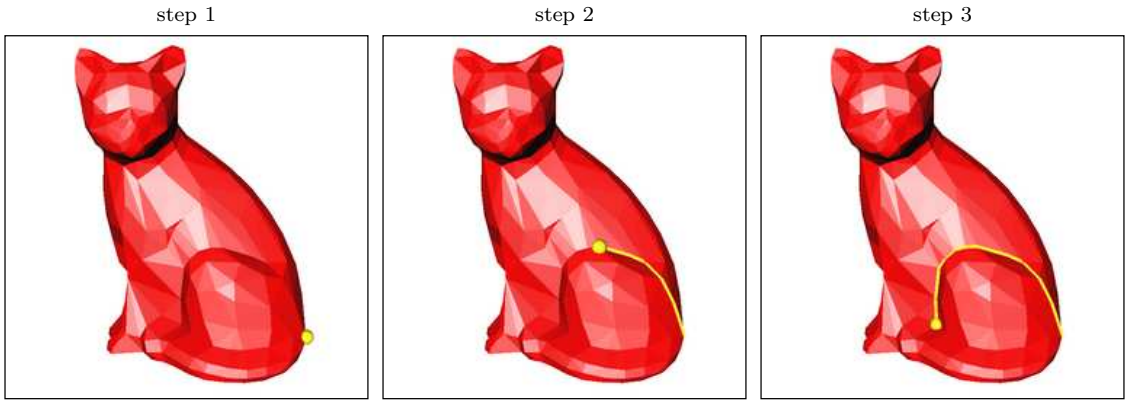

Figure 1: Specifying a segment boundary by three mouse clicks (marked by yellow spheres).

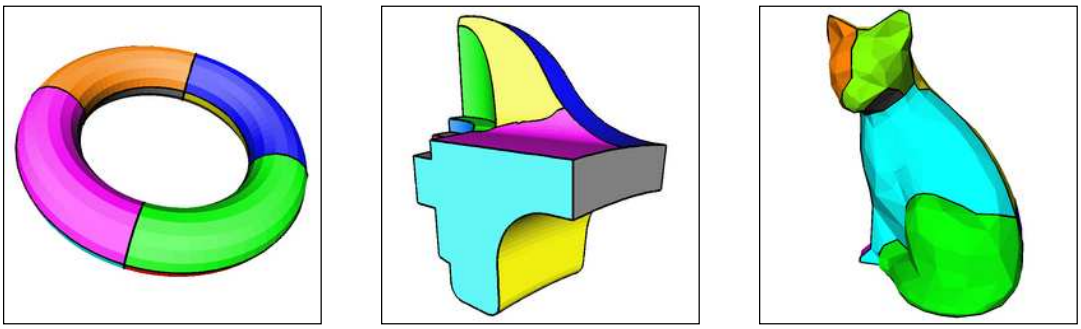

Figure 2: Triangle meshes, segmented with our tool.

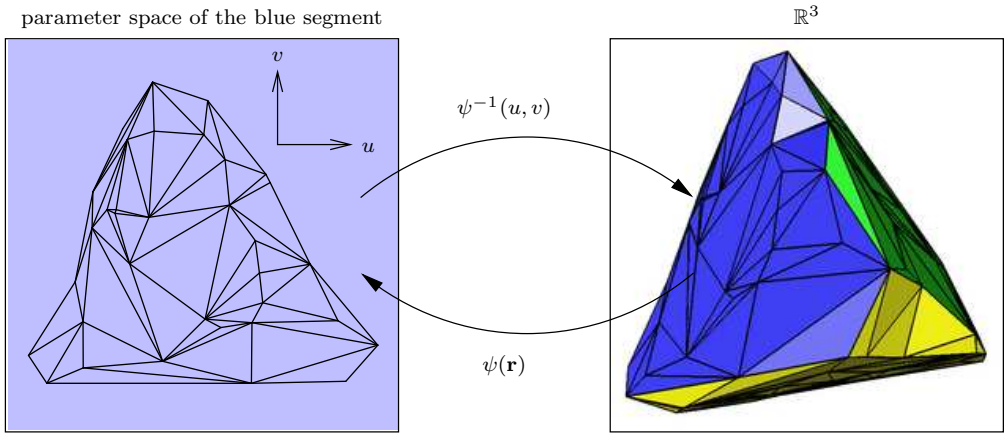

Figure 3: The parameterization of one of the segments of a deformed tetrahedron.

2.3 Approximating the segments with B-spline-surfaces

To approximate a parameterized segment with a visually pleasing surface we use the method of penalized least squares [GoSc88, Diet98, Floa98, Horm00]. The idea is to find the bicubic B-spline-surface

$$\mathbf{F}(u,v) \;=\; \sum_{i=0}^{p-1}\sum_{j=0}^{q-1} N_i^{3,\mathbf{U}}(u)\, N_j^{3,\mathbf{V}}(v)\, \mathbf{d}_{i,j}$$

with uniform knot vectors $\mathbf{U} = [t_{u,0}, \ldots, t_{u,p+3}]$, $t_{u,\alpha} = t_{u,0} + \alpha\Delta t_u$, and $\mathbf{V} = [t_{v,0}, \ldots, t_{v,q+3}]$, $t_{v,\beta} = t_{v,0} + \beta\Delta t_v$ that minimizes the functional

$$\mathcal{K}_\mu(\mathbf{F}) \;=\; \mathcal{E}(\mathbf{F}) + \mu\mathcal{J}(\mathbf{F})$$

which is a combination of the error functional $\mathcal{E}$,

$$\mathcal{E}(\mathbf{F}) \;=\; \sum_{k=1}^{N} \left(\mathbf{F}(u_k, v_k) - \mathbf{r}_k\right)^2 \quad ,$$

that measures the approximation error and the fairness functional $\mathcal{J}$,

$$\mathcal{J}(\mathbf{F}) \;=\; \int_{t_{u,3}}^{t_{u,p}} \int_{t_{v,3}}^{t_{v,q}} du\, dv\, \left((\mathbf{F}_{uu})^2 + 2(\mathbf{F}_{uv})^2 + (\mathbf{F}_{vv})^2\right) \quad ,$$

also known as the simplified thin plate energy.

The smoothing parameter μ controls the ratio between the approximation quality and the smoothness of the surface $\mathbf{F}$. A way of choosing this parameter automatically has been suggested in [Floa98]. The coefficients of the B-spline-surface can be found by solving a sparse linear system. Figure 4 shows an example where we have trimmed the B-spline-surfaces along the boundaries $\partial\psi(\mathcal{S}_i)$ of the parameterized segments.

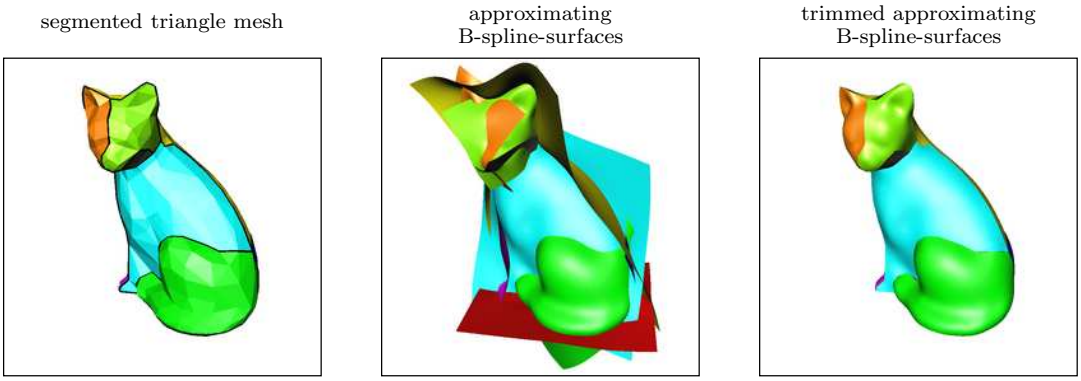

Figure 4: Approximation of a triangle mesh with B-spline-surfaces.

3 GENERATING C^2-CONTINUOUS RECONSTRUCTION SURFACES

Let us assume now that the given manifold triangle mesh has been decomposed into several segments and each of these segments has been parameterized and approximated by a bicubic C^2-continuous B-spline-surface, e. g. with the method described in the previous section.

3.1 Basic principle

The main idea of our method to create a C^2-continuous reconstruction surface is to smoothly blend the approximating B-spline-surfaces whenever their corresponding segments have a common boundary or a common vertex. In the regions near these common boundaries and common vertices we "cut back" the approximating B-spline-surfaces and insert *blending surfaces* that join C^2-continuously. The resulting reconstruction surface consists of several patches that can be classified in three different types:

Blending strips: Whenever two segments have a common boundary, the corresponding two approximating B-spline-surfaces are trimmed and smoothly (C^2-continuously) connected by a set of blending strips, one for each edge in the common boundary (see Figure 5; blending strips are coloured alternately red and light-red). Note that this set of blending strip "snippets" can later be combined into a single blending strip and that we treat them individually only for the purpose of simplifying the construction process.

N-surface-blends: Whenever $N \geq 3$ segments have a common vertex, the corresponding N approximating B-spline-surfaces and the adjacent N blending strips are smoothly (C^2-continuously) connected by an N-surface-blend (see Figure 5; N-surface-blends are coloured yellow).

Trimmed B-spline-surfaces: The interior regions of the segments are represented by the approximating B-spline-surfaces. These B-spline-surfaces are trimmed in a way, that they are smoothly (C^2-continuously) connected to their surrounding blending strips and N-surface-blends (see Figure 5; trimmed B-spline-surfaces are coloured blue).

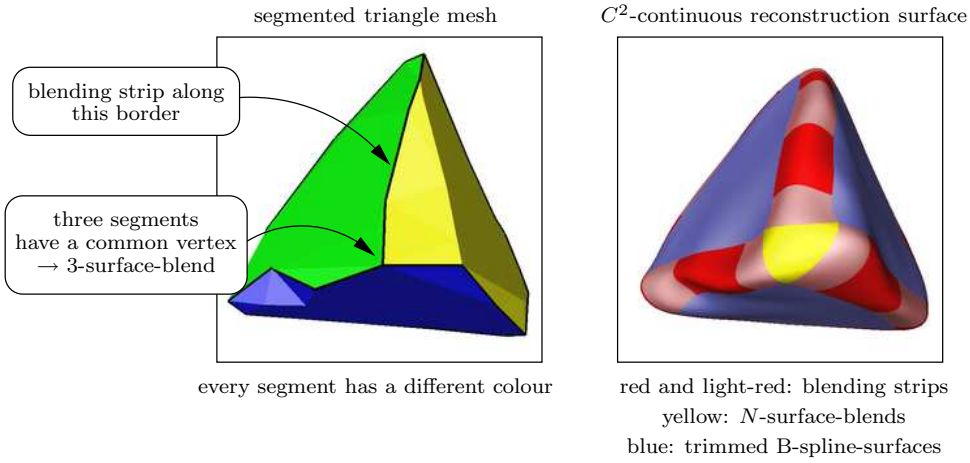

Figure 5: Segmented triangle mesh and reconstruction surface of a deformed tetrahedron.

3.2 C^2-continuous blending of two intersecting B-spline-surfaces

To illustrate our method and familiarize the reader with our notation, we first consider the simple example of blending two intersecting B-spline-surfaces $\mathbf{F}^{\downarrow} : D^{(u^{\downarrow},v^{\downarrow})} \to \mathbb{R}^3$ and $\mathbf{F}^{\uparrow} : D^{(u^{\uparrow},v^{\uparrow})} \to \mathbb{R}^3$. To further simplify the situation we assume that the B-spline surfaces are planes, intersecting each other at an angle of 90 degree (the red and green planes in the left part of Figure 6). However, bear in mind that everything that will be said can be applied to arbitrary pairs of B-spline-surfaces as well.

The basic idea is to cut off those parts of the B-spline-surfaces that are near the intersection curve and to fill the gap with a so called *blending strip* (lower part of Figure 6; the blending strip is coloured yellow). In the following we will discuss how to construct appropriate trimming curves for $\mathbf{F}^{\downarrow}$ and $\mathbf{F}^{\uparrow}$ and a blending strip so that the connections between the blending strip and the B-spline-surfaces are C^2-continuous.

The main difference between our and other blending methods is that we do not discard the parts of the B-spline-surfaces that we cut off and do not construct the blending strip based on the data along the boundaries of the two surfaces only. Instead we utilize the fact that $\mathbf{F}^{\downarrow}$ and $\mathbf{F}^{\uparrow}$ are also defined beyond the trimming curves. We define the blending strip by multiplying the B-spline-surfaces $\mathbf{F}^{\downarrow}$ and $\mathbf{F}^{\uparrow}$ with certain weight functions $H^{\downarrow}$ and $H^{\uparrow}$ and adding the results.

Since the B-spline-surfaces have independent parameter spaces $D^{(u^{\downarrow},v^{\downarrow})}$ and $D^{(u^{\uparrow},v^{\uparrow})}$ (the red and green rectangles in Figure 6), i. e., $\mathbf{F}^{\downarrow} = \mathbf{F}^{\downarrow}(u^{\downarrow}, v^{\downarrow})$ and $\mathbf{F}^{\uparrow} = \mathbf{F}^{\uparrow}(u^{\uparrow}, v^{\uparrow})$, we first establish a connection between these parameter spaces. We define two *parameter transformations* $\mathbf{G}^{\downarrow} : D^{(U,V)} \to D^{(u^{\downarrow},v^{\downarrow})}$ and $\mathbf{G}^{\uparrow} : D^{(U,V)} \to D^{(u^{\uparrow},v^{\uparrow})}$ that map a common quadratic parameter space $D^{(U,V)} = [0,1] \times [0,1]$ to parts of the parameter spaces $D^{(u^{\downarrow},v^{\downarrow})}$ and $D^{(u^{\uparrow},v^{\uparrow})}$ of the B-spline-surfaces. These parts (coloured in light red and light green in Figure 6) are called *blending regions* and encompass the inverse images of the intersection curve. In other words, the parameter transformations $\mathbf{G}^{\downarrow}$ and $\mathbf{G}^{\uparrow}$ are chosen such that the images $\mathbf{F}^{\downarrow}(\mathbf{G}^{\downarrow}(D^{(U,V)}))$ and $\mathbf{F}^{\uparrow}(\mathbf{G}^{\uparrow}(D^{(U,V)}))$ of the blending regions are close to the intersection curve of $\mathbf{F}^{\downarrow}$ and $\mathbf{F}^{\uparrow}$.

In the next step we use the interior boundaries of the blending regions to cut back the B-spline-surfaces. In other words, we use $\{\mathbf{G}^{\downarrow}(U,0), U \in [0,1]\} \subset D^{(u^{\downarrow},v^{\downarrow})}$ as a trimming curve for $\mathbf{F}^{\downarrow}$ and $\{\mathbf{G}^{\uparrow}(U,1), U \in [0,1]\} \subset D^{(u^{\uparrow},v^{\uparrow})}$ as a trimming curve for $\mathbf{F}^{\uparrow}$.

We choose the weight functions $H^{\downarrow} : D^{(U,V)} \to [0,1]$ and $H^{\uparrow} : D^{(U,V)} \to [0,1]$ (the cyan height fields in Figure 6), also called *blending functions*, to be scalar functions, satisfying $H^{\downarrow} + H^{\uparrow} = 1$, i. e., they are suitable weights for a convex combination.

We are now in a position to define the blending strip as a combination of the B-spline-surfaces, the parameter transformations, and the blending functions,

$$\mathcal{F}_{\mathrm{bs}}(U,V) \;=\; H^{\downarrow}(U,V) \cdot \mathbf{F}^{\downarrow}(\mathbf{G}^{\downarrow}(U,V)) \,+\, H^{\uparrow}(U,V) \cdot \mathbf{F}^{\uparrow}(\mathbf{G}^{\uparrow}(U,V)) \quad . \tag{2}$$

This equation is illustrated graphically in Figure 6.

To guarantee C^2-continuity between the blending strip and the B-spline-surfaces we require $H^{\downarrow}(U,0) = 1$ and $H^{\downarrow}(U,1) = 0$ for $U \in [0,1]$ (and vice versa for $H^{\uparrow}$) and the first and second derivatives of $H^{\downarrow}$ and $H^{\uparrow}$ to disappear there.

3.3 Generating closed C^2-continuous reconstruction surfaces

We will now generalize the concept explained in the previous section to create a C^2-continuous reconstruction surface from a set of B-spline-surfaces that approximate the segments of a closed manifold triangle mesh. As mentioned in Section 2.1, our reconstruction surface will consist

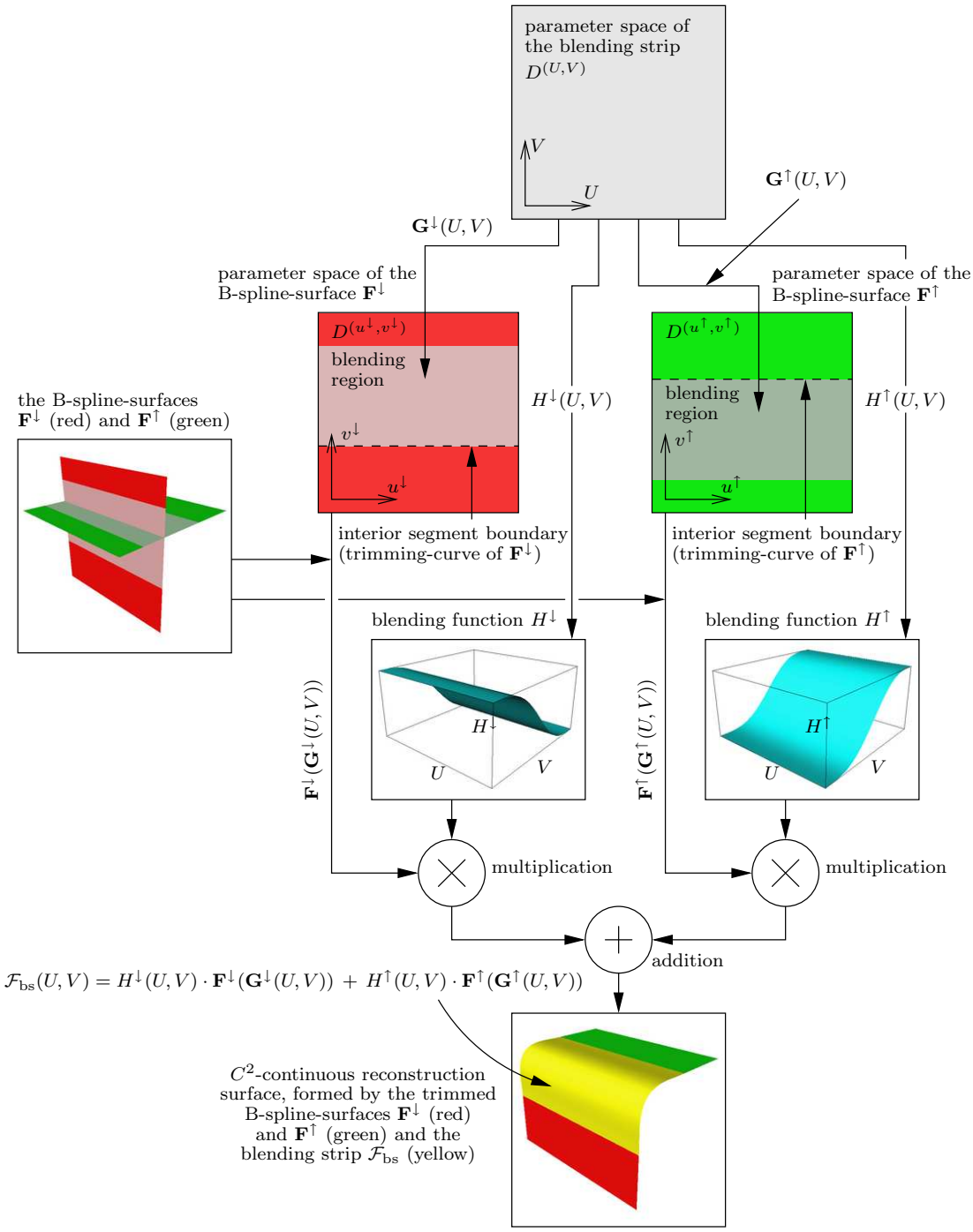

Figure 6: C^2-continuous blending of two intersecting B-spline-surfaces.

of patches of three different types: blending strips, N-surface-blends, and trimmed B-spline-surfaces.

Whenever two segments have a common boundary, we cut off parts of the corresponding B-spline-surfaces and insert a set of blending strips, one for each edge in the common boundary (see Figure 5; blending strips are coloured alternately red and light-red). These blending strips

are constructed as explained in the previous section.

The upper part of Figure 7 (solid lines) shows in detail how one of the blending strips $\mathcal{F}_{\text{bs}}$ of the reconstruction surface of a deformed tetrahedron is created. The common parameter space $D^{(U,V)}$ is mapped to the parameter spaces $D^{(u^1,v^1)}$ and $D^{(u^2,v^2)}$ of the two corresponding B-spline-surfaces $\mathbf{F}^1$ and $\mathbf{F}^2$ by the parameter transformations $\mathbf{G}^{\downarrow}$ and $\mathbf{G}^{\uparrow}$. This establishes a connection between the parameter spaces and allows us to add the B-spline-surfaces $\mathbf{F}^1$ and $\mathbf{F}^2$ after multiplying them with the blending functions $H^{\downarrow}$ and $H^{\uparrow}$. This defines the blending strip

$$\mathcal{F}_{\text{bs}}(U,V) \;=\; H^{\downarrow}(U,V)\cdot\mathbf{F}^1(\mathbf{G}^{\downarrow}(U,V)) \,+\, H^{\uparrow}(U,V)\cdot\mathbf{F}^2(\mathbf{G}^{\uparrow}(U,V)) \quad ,$$

shown in the upper part of Figure 7. Note that this definition is equivalent to the general form of a blending strip (see Equation (2)) after renaming the indices of the B-spline-surfaces.

Whenever $N \geq 3$ segments have a common vertex, we replace parts of the corresponding B-spline-surfaces by an N-surface-blend (see Figure 5; N-surface-blends are coloured yellow). The construction of N-surface-blends is very similar to the construction of blending strips. The parameter space $D^{(U,V)}$ of an N-surface-blend is a regular N-gon with edge length 1. We chose this particular parameter space because it has an N-fold rotational symmetry around the center, which is necessary for a symmetric treatment of the N corresponding B-spline-surfaces. In complete analogy to the construction of the blending strips we define parameter transformations $\mathbf{G}^i : D^{(U,V)} \rightarrow D^{(u^i,v^i)}$, $i = 1,\ldots,N$ to establish connections between the independent parameter spaces $D^{(u^i,v^i)}$ of the B-spline-surfaces $\mathbf{F}^i$ and blending functions $H^{N,i} : D^{(U,V)} \rightarrow [0,1]$, $i = 1,\ldots,N$. We also enforce certain interpolation constraints on the blending functions along the boundary of $D^{(U,V)}$ so as to assure C^2-continuity between the N-surface-blend and the N adjacent blending strips. The general form of an N-surface-blend is then given by

$$\mathcal{F}_{N\text{sb}}(U,V) \;=\; \sum_{i=1}^{N} H^{N,i}(U,V)\cdot\mathbf{F}^i(\mathbf{G}^i(U,V)) \quad . \tag{3}$$

The lower part of Figure 7 (dashed lines) shows in detail how one of the 3-surface-blends $\mathcal{F}_{3\text{sb}}$ of the reconstruction surface of a deformed tetrahedron is created. The common parameter space $D^{(U,V)}$ is mapped to the parameter spaces $D^{(u^2,v^2)}$, $D^{(u^3,v^3)}$, and $D^{(u^4,v^4)}$ of the three corresponding B-spline-surfaces $\mathbf{F}^2$, $\mathbf{F}^3$, and $\mathbf{F}^4$ by the parameter transformations $\mathbf{G}^1$, $\mathbf{G}^2$, and $\mathbf{G}^3$. This establishes a connection between the parameter spaces and allows us to add the B-spline-surfaces $\mathbf{F}^2$, $\mathbf{F}^3$, and $\mathbf{F}^4$ after multiplying them with the blending functions $H^{3,1}$, $H^{3,2}$, and $H^{3,3}$. This defines the 3-surface-blend

$$\begin{aligned}\mathcal{F}_{3\text{sb}}(U,V) \;=\;& H^{3,1}(U,V)\cdot\mathbf{F}^2(\mathbf{G}^1(U,V)) \,+\, H^{3,2}(U,V)\cdot\mathbf{F}^3(\mathbf{G}^2(U,V)) \,+\\ & H^{3,3}(U,V)\cdot\mathbf{F}^4(\mathbf{G}^3(U,V)) \quad ,\end{aligned}$$

shown in the lower part of Figure 7. Note that this definition is equivalent to the general form of a 3-surface-blend (see Equation (3) with $N = 3$) after renaming the indices of the B-spline-surfaces.

The trimming curves for the B-spline-surfaces are the interior boundaries of their blending regions. The blending regions are the ring-like regions defined by the parameter transformations of all blending-strips and N-surface-blends (the blending regions are coloured light-red, light-blue, light-yellow and light-green in the parameter spaces $D^{(u^1,v^1)},\ldots,D^{(u^4,v^4)}$ in Figure 7). The trimming curves can be obtained by inserting the corresponding boundaries of the parameter spaces of the blending strips into their parameter transformations (see Figure 7; the parameter space $D^{(u^4,v^4)}$ of the green B-spline-surface).

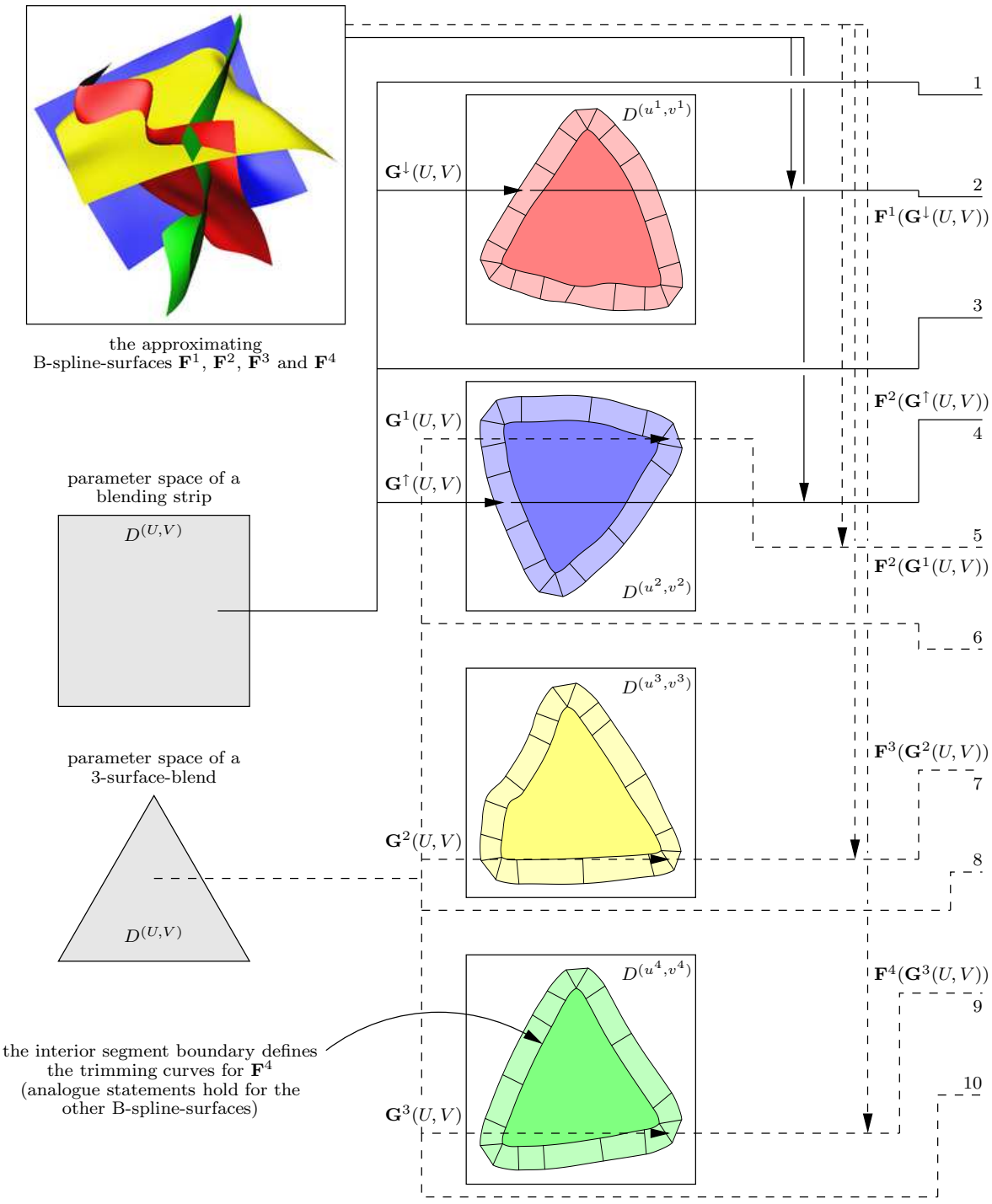

Figure 7: C^2-continuous reconstruction of a deformed tetrahedron (left part)

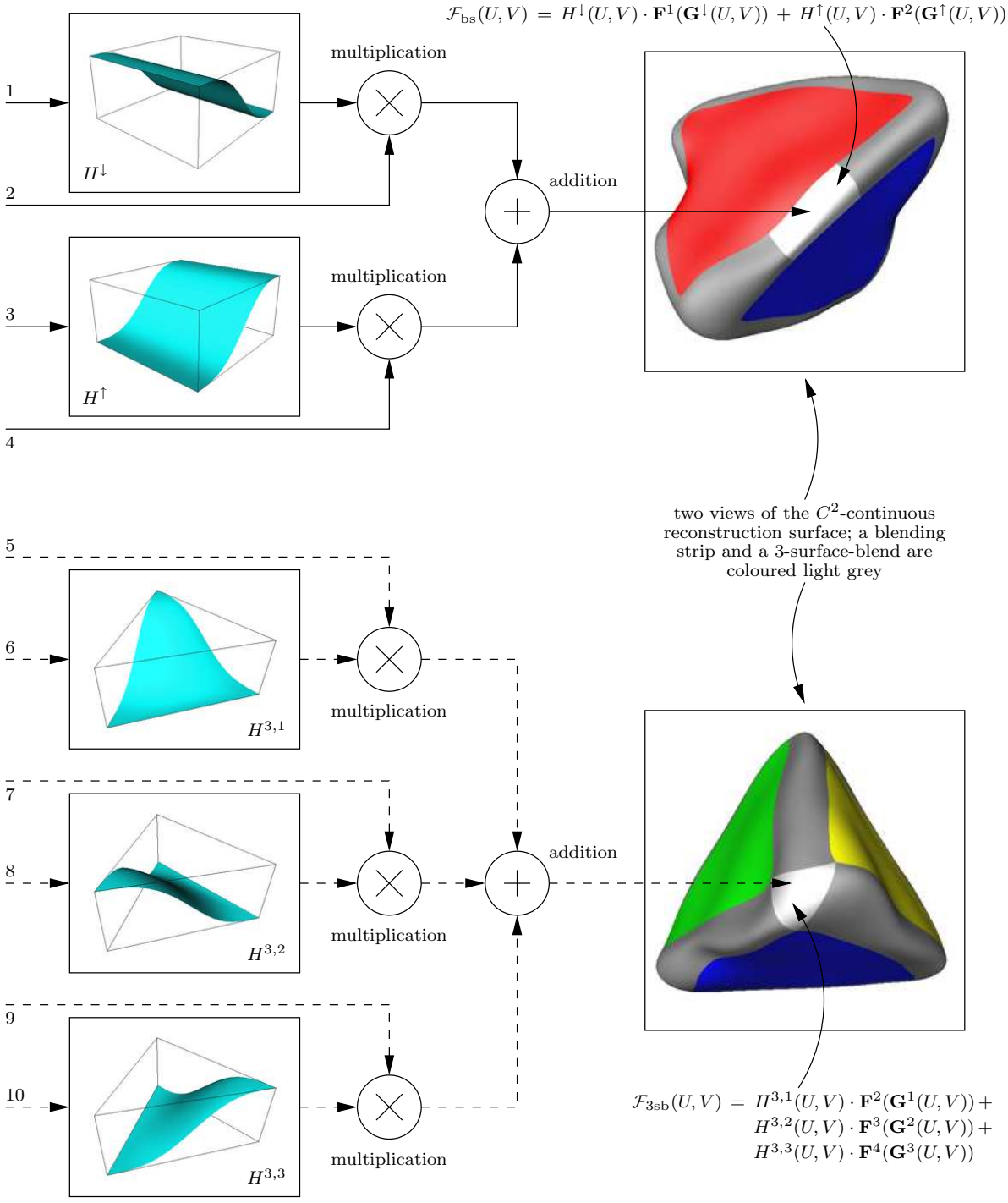

Figure 7: C^2-continuous reconstruction of a deformed tetrahedron (right part)

Until now we did not explicitely say how to construct suitable parameter transformations $\mathbf{G}^{\downarrow}$, $\mathbf{G}^{\uparrow}$, and $\mathbf{G}^{i}$ and blending functions $H^{\downarrow}$, $H^{\uparrow}$, and $H^{N,i}$. So far we have only outlined the rather simple and basic principle of our method. But the construction of proper parameter transformations and blending functions is a little bit more involved and we will discuss it in detail in the following sections.

4 C^2-CONDITIONS FOR THE RECONSTRUCTION SURFACE

In this section we discuss which conditions the parameter transformations $\mathbf{G}^{\downarrow}$, $\mathbf{G}^{\uparrow}$, and $\mathbf{G}^{i}$ and the blending functions $H^{\downarrow}$, $H^{\uparrow}$, and $H^{N,i}$ have to fulfill so that the reconstruction surface is C^2-continuous.

Keep in mind that we do not want the blending functions to depend on a specific blending strip or N-surface blend. We rather want to construct them in a general way so that they can be applied to every blending strip or N-surface blend of any reconstruction surface. In contrast to that, the parameter transformations will be constructed individually for every blending surface.

We derive the conditions in a rather abstract way in order to keep them as general as possible. They do not depend on a specific function type chosen to describe the parameter transformations and the blending functions. In other words, our method is not specifically designed for polynomials (although we use polynomials throughout this report) but can also be applied to arbitrary classes of functions. Readers who are not interested in the mathematical details can skip the major part of this section but should at least take a look at the resulting conditions (H1) to (H18) and (G1) to (G8) and their geometric interpretation given in the last paragraphs of Sections 4.2.1 to 4.2.3.

4.1 C^2-conditions for patch interiors

The bicubic B-spline-surfaces that are used to approximate the interior regions of the segments are C^2-continuous by construction.

It follows from the definition of the blending strips

$$\mathcal{F}_{\mathrm{bs}}(U,V) \;=\; H^{\downarrow}(U,V)\cdot\mathbf{F}^{\downarrow}(\mathbf{G}^{\downarrow}(U,V)) \;+\; H^{\uparrow}(U,V)\cdot\mathbf{F}^{\uparrow}(\mathbf{G}^{\uparrow}(U,V))$$

and the definition of the N-surface-blends

$$\mathcal{F}_{N\mathrm{sb}}(U,V) \;=\; \sum_{i=1}^{N} H^{N,i}(U,V)\cdot\mathbf{F}^{i}(\mathbf{G}^{i}(U,V))$$

that these patches are C^2-continuous if the parameter transformations $\mathbf{G}^{\downarrow}$, $\mathbf{G}^{\uparrow}$, and $\mathbf{G}^{i}$ and the blending functions $H^{\downarrow}$, $H^{\uparrow}$, and $H^{N,i}$ are C^2-continuous (compositions of functions are C^k-continuous if their components are C^k-continuous).

4.2 C^2-conditions for patch boundaries

There are three different situations that occur at the boundary of the patches: a blending strip connecting to one of the two B-spline-surfaces that it blends, a blending strip connecting to another neighbouring blending strip, and a blending strip connecting to an N-surface-blend. We analyse the continuity in the different settings with the aid of properly chosen charts, which is the common way in differential geometry.

4.2.1 Continuity between a blending strip and its adjacent B-spline-surfaces

The topology and the charts we use to analyse this situation are shown in Figure 8. The blending

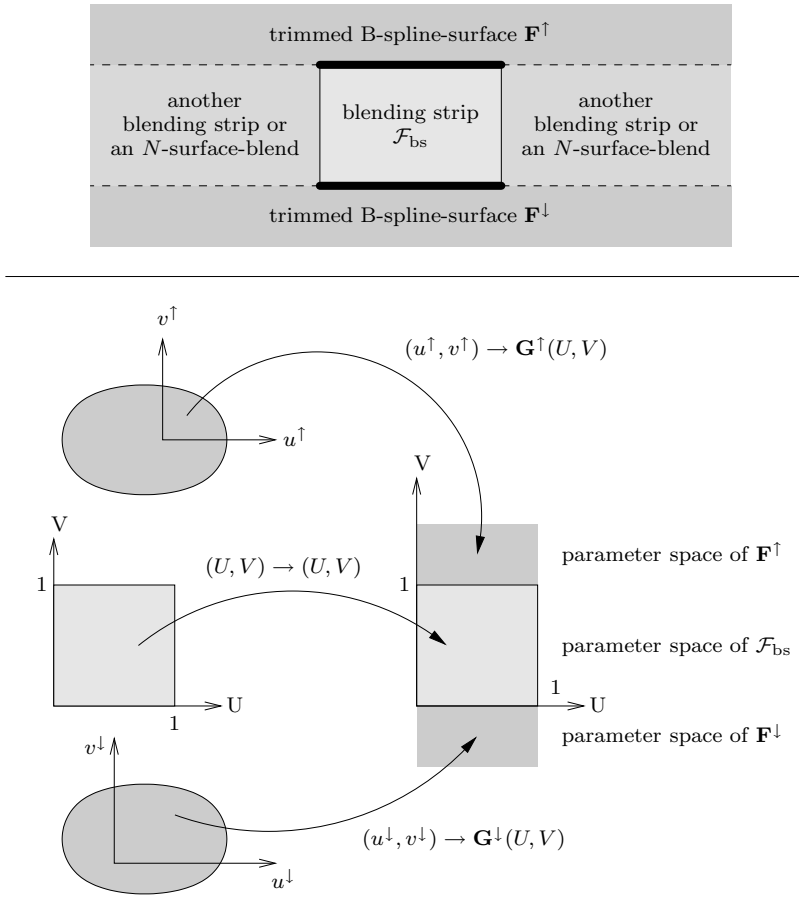

Figure 8: Topology and charts for analysing the continuity between a blending strip and its adjacent B-spline-surfaces.

strip $\mathcal{F}_{\text{bs}}$ is given by

$$\mathcal{F}_{\text{bs}}(U,V) \;=\; H^{\downarrow}(U,V) \cdot \mathbf{F}^{\downarrow}(\mathbf{G}^{\downarrow}(U,V)) \;+\; H^{\uparrow}(U,V) \cdot \mathbf{F}^{\uparrow}(\mathbf{G}^{\uparrow}(U,V)) \tag{4}$$

and we do not reparameterize it since we take its parameter space $D^{(U,V)}$ as the reference domain. The reparameterizations $(u^{\downarrow}, v^{\downarrow}) \rightarrow \mathbf{G}^{\downarrow}(U,V)$ and $(u^{\uparrow}, v^{\uparrow}) \rightarrow \mathbf{G}^{\uparrow}(U,V)$ for the trimmed B-spline-surfaces $\mathbf{F}^{\downarrow}$ and $\mathbf{F}^{\uparrow}$ yield

$$\mathbf{F}^{\downarrow}(u^{\downarrow}, v^{\downarrow}) \;\rightarrow\; \mathbf{F}^{\downarrow}(\mathbf{G}^{\downarrow}(U,V)) \tag{5}$$

$$\mathbf{F}^{\uparrow}(u^{\uparrow}, v^{\uparrow}) \;\rightarrow\; \mathbf{F}^{\uparrow}(\mathbf{G}^{\uparrow}(U,V)) \tag{6}$$

($A \rightarrow B$ stands for A is replaced by B). In other words, we use the parameter transformation $\mathbf{G}^{\downarrow}(U,V)$ to map the reference domain $D^{(U,V)}$ to the parameter space $D^{(u^{\downarrow},v^{\downarrow})}$ over which the surface $\mathbf{F}^{\downarrow}(u^{\downarrow}, v^{\downarrow})$ is defined and then interpret $\mathbf{F}^{\downarrow}$ as being defined over $D^{(U,V)}$ instead (likewise for $\mathbf{F}^{\uparrow}$).

The surfaces $\mathcal{F}_{\text{bs}}$ and $\mathbf{F}^{\downarrow}$ meet along the line $(U,0)$, $U \in [0,1]$ and are C^2-continuous if and only if the function values and the first and second derivatives at this line are equal. Equating the right-hand sides of (4) and (5), deriving sufficiently often, and comparing coefficients gives

conditions for $H^{\downarrow}$ and $H^{\uparrow}$,

$$\frac{\partial^\alpha}{\partial U^\alpha}\frac{\partial^\beta}{\partial V^\beta}H^{\downarrow}(U,0) \;=\; \delta_{\alpha,0}\,\delta_{\beta,0} \quad,\quad \alpha=0,\ldots,2 \quad,\quad \beta=0,\ldots,2-\alpha \quad,$$
$$\frac{\partial^\alpha}{\partial U^\alpha}\frac{\partial^\beta}{\partial V^\beta}H^{\uparrow}(U,0) \;=0 \quad,\quad \alpha=0,\ldots,2 \quad,\quad \beta=0,\ldots,2-\alpha \quad,$$

that can be simplified to

(H1)	$H^{\downarrow}(U,0) = 1$	(H7)	$H^{\uparrow}(U,0) = 0$
(H2)	$H^{\downarrow}_V(U,0) = 0$	(H8)	$H^{\uparrow}_V(U,0) = 0$
(H3)	$H^{\downarrow}_{VV}(U,0) = 0$	(H9)	$H^{\uparrow}_{VV}(U,0) = 0$.

Equating the right-hand sides of (4) and (6) along the line $(U,1)$, $U\in[0,1]$ leads to a similar set of conditions,

(H4)	$H^{\downarrow}(U,1) = 0$	(H10)	$H^{\uparrow}(U,1) = 1$
(H5)	$H^{\downarrow}_V(U,1) = 0$	(H11)	$H^{\uparrow}_V(U,1) = 0$
(H6)	$H^{\downarrow}_{VV}(U,1) = 0$	(H12)	$H^{\uparrow}_{VV}(U,1) = 0$.

Geometric interpretation of (H1) to (H12)

(H1), (H4), (H7), and (H10) guarantee that the resulting blending strips match their corresponding B-spline-surfaces along the lines $(U,0)$ and $(U,1)$, $U\in[0,1]$. The remaining conditions assure that the blending functions take on their values at these lines smoothly, i. e., the function that is constant zero and the function that is constant one are C^2-continuous continuations. Consequently, the connections between the blending strips and the trimmed B-spline-surfaces of the reconstruction surface are C^2-continuous as well.

4.2.2 Continuity between two blending strips

The topology and the charts for this situation are shown in Figure 9. In order to parameterize the blending strips $\mathcal{F}_{\text{bs}}$ and $\tilde{\mathcal{F}}_{\text{bs}}$ over a common reference domain, we use the linear reparameterizations $(U,V)\to(\frac{U}{a}+1,V)$ and $(U,V)\to(\frac{U}{\tilde a},V)$ that yield

$$\mathcal{F}_{\text{bs}}(U,V) \;\to\; H^{\downarrow}(\frac{U}{a}+1,V)\cdot\mathbf{F}^{\downarrow}(\mathbf{G}^{\downarrow}(\frac{U}{a}+1,V)) \;+\; H^{\uparrow}(\frac{U}{a}+1,V)\cdot\mathbf{F}^{\uparrow}(\mathbf{G}^{\uparrow}(\frac{U}{a}+1,V)) \qquad (7)$$
$$\tilde{\mathcal{F}}_{\text{bs}}(U,V) \;\to\; H^{\downarrow}(\frac{U}{\tilde a},V)\cdot\mathbf{F}^{\downarrow}(\tilde{\mathbf{G}}^{\downarrow}(\frac{U}{\tilde a},V)) \;+\; H^{\uparrow}(\frac{U}{\tilde a},V)\cdot\mathbf{F}^{\uparrow}(\tilde{\mathbf{G}}^{\uparrow}(\frac{U}{\tilde a},V)) \quad . \qquad (8)$$

The scalars a and $\tilde a$ are additional degrees of freedom that can be chosen individually for every pair of neighbouring blending strips. We will use them during the construction of the parameter transformations in Section 6 to improve the shape of the reconstruction surface.

The blending strips $\mathcal{F}_{\text{bs}}$ and $\tilde{\mathcal{F}}_{\text{bs}}$ meet along the line $(0,V)$, $V\in[0,1]$ and are C^2-continuous if and only if the function values and the first and second derivatives are equal. Equating the right-hand sides of (7) and (8), deriving sufficiently often, and comparing coefficients gives conditions for $H^{\downarrow}$ and $H^{\uparrow}$,

$$\frac{\partial^\alpha}{\partial U^\alpha}\frac{\partial^\beta}{\partial V^\beta}H^{i}(1,V)\,\frac{1}{a^\alpha} \;=\; \frac{\partial^\alpha}{\partial U^\alpha}\frac{\partial^\beta}{\partial V^\beta}H^{i}(0,V)\,\frac{1}{\tilde a^\alpha} \quad,\quad \alpha=0,\ldots,2 \quad,\quad \beta=0,\ldots,2-\alpha \quad,$$
$$i=\downarrow,\uparrow$$

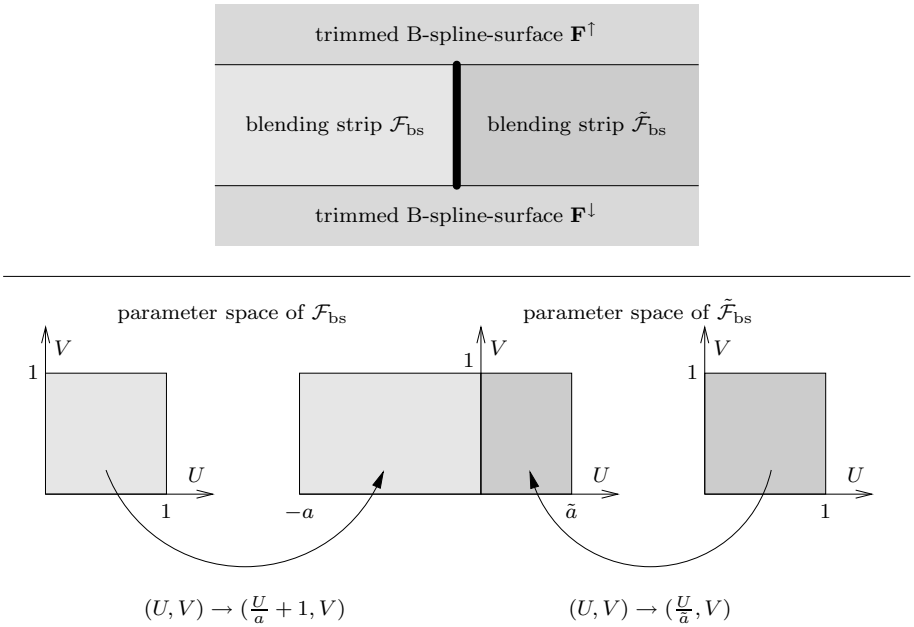

Figure 9: Topology and charts for analysing the continuity between two blending strips.

that can be simplified to

$$\begin{aligned}
&\text{(H13)} \quad H^i(1,V) \;=\; H^i(0,V)\\
&\text{(H14)} \quad H^i_U(1,V) \;=\; H^i_U(0,V) \;=\; 0\\
&\text{(H15)} \quad H^i_{UU}(1,V) \;=\; H^i_{UU}(0,V) \;=\; 0 \quad , \quad i = \downarrow, \uparrow \quad ,
\end{aligned}$$

and conditions for $\mathbf{G}^{\downarrow}$ and $\mathbf{G}^{\uparrow}$,

$$\frac{\partial^\alpha}{\partial U^\alpha}\frac{\partial^\beta}{\partial V^\beta}\mathbf{G}^i(1,V)\frac{1}{a^\alpha} \;=\; \frac{\partial^\alpha}{\partial U^\alpha}\frac{\partial^\beta}{\partial V^\beta}\tilde{\mathbf{G}}^i(0,V)\frac{1}{\tilde{a}^\alpha} \quad , \quad \alpha = 0,\ldots,2 \quad , \quad \beta = 0,\ldots,2-\alpha \quad , \quad i = \downarrow, \uparrow \quad ,$$

that can be simplified to

$$\begin{aligned}
&\text{(G1)} \quad \mathbf{G}^i(1,V) \;=\; \tilde{\mathbf{G}}^i(0,V)\\
&\text{(G2)} \quad \mathbf{G}^i_U(1,V)\frac{1}{a} \;=\; \tilde{\mathbf{G}}^i_U(0,V)\frac{1}{\tilde{a}}\\
&\text{(G3)} \quad \mathbf{G}^i_{UU}(1,V)\frac{1}{a^2} \;=\; \tilde{\mathbf{G}}^i_{UU}(0,V)\frac{1}{\tilde{a}^2}\\
&\text{(G4)} \quad \mathbf{G}^i_{UV}(1,V)\frac{1}{a} \;=\; \tilde{\mathbf{G}}^i_{UV}(0,V)\frac{1}{\tilde{a}} \quad , \quad i = \downarrow, \uparrow \quad .
\end{aligned}$$

Geometric interpretation of (H13) to (H15) and (G1) to (G4)

The geometric meaning of conditions (H13) to (H15) and (G1) to (G4) is that the blending functions and the parameter transformations have to join C^2-continuously. The linear reparameterizations with the parameters a and $\tilde{a}$ refer to the fact that there is no difference between surfaces of parametric continuity and surfaces of geometric continuity if only the shapes of the

surfaces are of interest. By permitting these linear reparameterizations we gain another degree of freedom for every pair of neighbouring blending strips. It will be used during the construction of the parameter transformations to improve the shape of the reconstruction surface.

4.2.3 Continuity between an N-surface-blend and its adjacent blending strips

The topology and the charts for this situation are shown in Figure 10. We do not reparameterize the N-surface-blend $\mathcal{F}_{N\mathrm{sb}}$ that is given by

$$\mathcal{F}_{N\mathrm{sb}}(U,V) \quad = \quad \sum_{i=1}^{N} H^{N,i}(U,V) \cdot \mathbf{F}^i(\mathbf{G}^i(U,V)) \tag{9}$$

and for the blending strips $\mathcal{F}_{\mathrm{bs}}^{k,j}$ we use the same linear reparameterizations $(U,V) \rightarrow (\frac{U}{a},V)$ that we have already seen in the previous section. It yields

$$\begin{aligned} \mathcal{F}_{\mathrm{bs}}^{k,j}(U,V) \quad &\rightarrow \quad H^{\downarrow}(\frac{U}{a},V) \cdot \mathbf{F}^k(\mathbf{G}^{k,\downarrow}(\frac{U}{a},V)) \; + \; H^{\uparrow}(\frac{U}{a},V) \cdot \mathbf{F}^j(\mathbf{G}^{j,\uparrow}(\frac{U}{a},V)) \quad , \\ & j = 1,\ldots,N \quad , \quad k = (j \bmod N) + 1 \quad . \end{aligned} \tag{10}$$

The scalar a is a degree of freedom that can be chosen individually for every N-surface blend. Note that we do not further rotate and translate the parameter spaces of the blending strips in order to align them with the parameter space of the N-surface-blend, i. e. we do not represent the N-surface-blend and its adjacent blending strips in a common reference domain. Instead, we keep all patches in their local coordinate systems and rather use directional derivatives to analyse the continuity between $\mathcal{F}_{\mathrm{bs}}^{k,j}$ and $\mathcal{F}_{N\mathrm{sb}}$. The directional derivative of a function $\mathbf{F}$ at a point (U_0,V_0) in direction $\mathbf{e}$, $\|\mathbf{e}\| = 1$ is defined as

$$\mathbf{F}_{\mathbf{e}}(U_0,V_0) \quad \equiv \quad \frac{\partial}{\partial \mathbf{e}} \mathbf{F}(U_0,V_0) \quad = \quad \langle \mathbf{grad}\, \mathbf{F}(U_0,V_0)\,,\, \mathbf{e} \rangle \quad .$$

In the following we denote the line where the blending strip $\mathcal{F}_{\mathrm{bs}}^{k,j}$ and the N-surface-blend $\mathcal{F}_{N\mathrm{sb}}$ meet by $\mathcal{E}^{k,j}$ (see Figure 10). Let $\mathbf{e}_{\parallel}^{k,j}$ be the unit vector parallel to $\mathcal{E}^{k,j}$ oriented clockwise relative to the N-gonal parameter space of $\mathcal{F}_{N\mathrm{sb}}$ and let $\mathbf{e}_{\perp}^{k,j}$ be the unit vector perpendicular to $\mathcal{E}^{k,j}$ pointing at the center of the N-gonal parameter space of $\mathcal{F}_{N\mathrm{sb}}$. Between the directional derivatives and the U- and $V-$derivatives of the blending strip the simple but useful relation

$$\frac{\partial^\alpha}{(\partial \mathbf{e}_{\perp}^{k,j})^\alpha} \frac{\partial^\beta}{(\partial \mathbf{e}_{\parallel}^{k,j})^\beta} \mathcal{F}_{\mathrm{bs}}^{k,j}(U,V) \quad = \quad \frac{\partial^\alpha}{\partial U^\alpha} \frac{\partial^\beta}{\partial V^\beta} \mathcal{F}_{\mathrm{bs}}^{k,j}(U,V) \tag{11}$$

holds. The surfaces $\mathcal{F}_{N\mathrm{sb}}$ and $\mathcal{F}_{\mathrm{bs}}^{k,j}$ are C^2-continuous along the line $\mathcal{E}^{k,j}$ if and only if the function values and the first and second derivatives are equal. Equating the right-hand sides of (9) and (10), deriving sufficiently often with respect to $\mathbf{e}_{\parallel}^{k,j}$ and $\mathbf{e}_{\perp}^{k,j}$, using (11), and comparing coefficients gives conditions for the blending functions,

$$\begin{aligned} \frac{\partial^\alpha}{(\partial \mathbf{e}_{\perp}^{k,j})^\alpha} \frac{\partial^\beta}{(\partial \mathbf{e}_{\parallel}^{k,j})^\beta} H^{N,i}(\mathcal{E}^{k,j}) \quad &= \quad \delta_{i,k} \cdot \frac{\partial^\alpha}{\partial U^\alpha} \frac{\partial^\beta}{\partial V^\beta} H^{\downarrow}(1,V) \frac{1}{a^\alpha} \; + \; \delta_{i,j} \cdot \frac{\partial^\alpha}{\partial U^\alpha} \frac{\partial^\beta}{\partial V^\beta} H^{\uparrow}(1,V) \frac{1}{a^\alpha} \\ & \alpha = 0,\ldots,2 \quad , \quad \beta = 0,\ldots,2-\alpha \quad , \quad i = 1,\ldots,N \quad , \quad j = 1,\ldots,N \quad , \\ & k = (j \bmod N) + 1 \quad , \end{aligned}$$

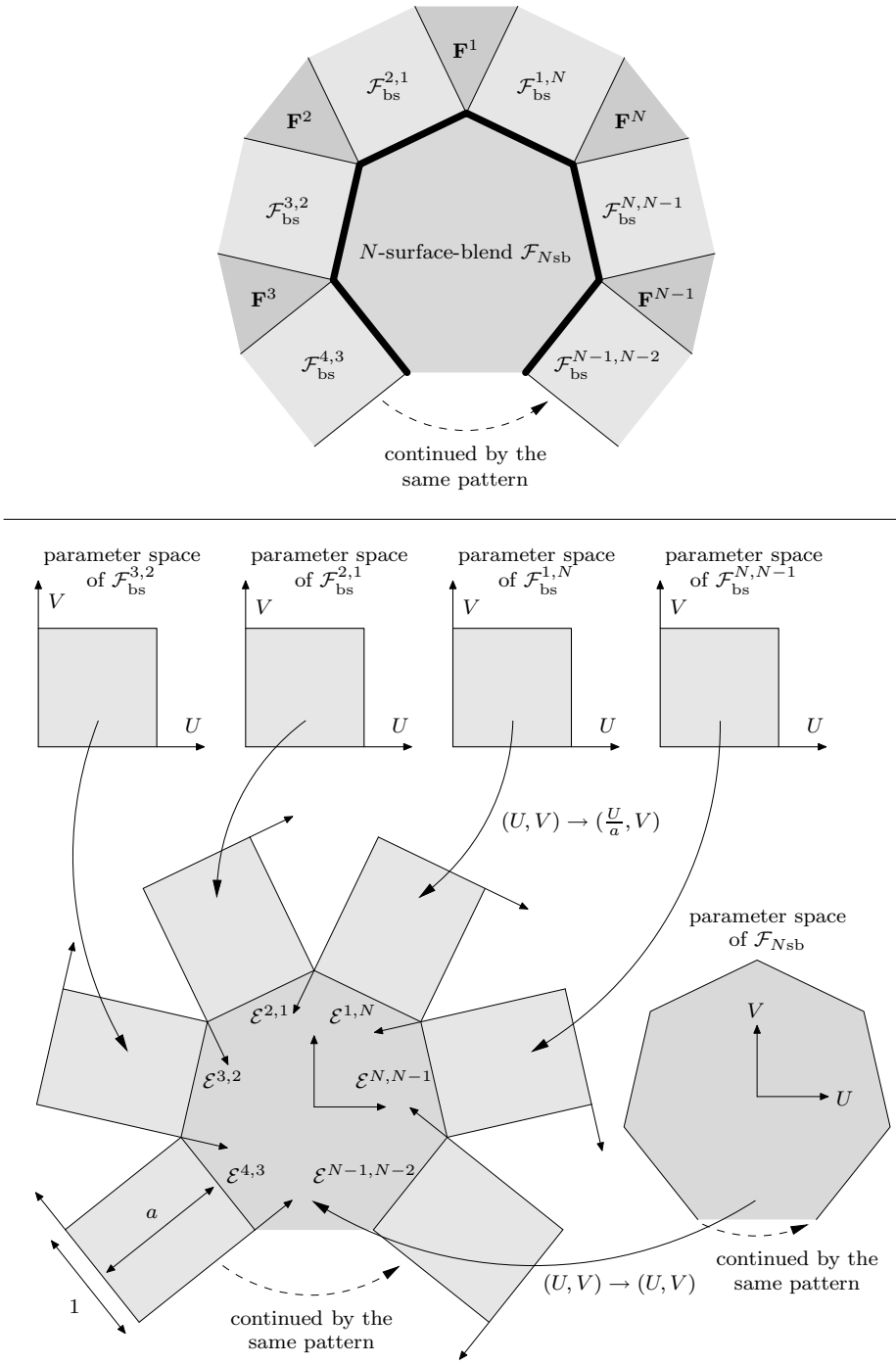

Figure 10: Topology and charts for analysing the continuity between an N-surface-blend and its adjacent blending strips.

that can be simplified to

(H16) $$H^{N,i}(\mathcal{E}^{k,j}) = \delta_{i,k} \cdot H^{\downarrow}(1,V) + \delta_{i,j} \cdot H^{\uparrow}(1,V)$$

(H17) $$H^{N,i}_{\mathbf{e}^{k,j}_{\perp}}(\mathcal{E}^{k,j}) = 0$$

$$\text{(H18)} \qquad H^{N,i}_{\mathbf{e}_\perp^{k,j}\mathbf{e}_\perp^{k,j}}(\mathcal{E}^{k,j}) \;=\; 0 \quad , \quad i=1,\dots,N \quad , \quad j=1,\dots,N \quad , \quad k=(j \bmod N)+1 \quad ,$$

and conditions for the parameter transformations,

$$\frac{\partial^\alpha}{(\partial \mathbf{e}_\perp^{k,j})^\alpha}\frac{\partial^\beta}{(\partial \mathbf{e}_\parallel^{k,j})^\beta}\mathbf{G}^i(\mathcal{E}^{k,j}) \;=\; \delta_{i,k}\cdot\frac{\partial^\alpha}{\partial U^\alpha}\frac{\partial^\beta}{\partial V^\beta}\mathbf{G}^{i,\downarrow}(1,V)\,\frac{1}{a^\alpha} \;+\; \delta_{i,j}\cdot\frac{\partial^\alpha}{\partial U^\alpha}\frac{\partial^\beta}{\partial V^\beta}\mathbf{G}^{i,\uparrow}(1,V)\,\frac{1}{a^\alpha}$$
$$\alpha=0,\dots,2 \quad , \quad \beta=0,\dots,2-\alpha \quad , \quad j=1,\dots,N \quad , \quad k=(j \bmod N)+1 \quad , \quad i=j,k \quad ,$$

that can be simplified to

$$\text{(G5)} \qquad \mathbf{G}^i(\mathcal{E}^{k,j}) \;=\; \delta_{i,k}\cdot\mathbf{G}^{i,\downarrow}(1,V) \;+\; \delta_{i,j}\cdot\mathbf{G}^{i,\uparrow}(1,V)$$

$$\text{(G6)} \qquad \mathbf{G}^i_{\mathbf{e}_\perp^{k,j}}(\mathcal{E}^{k,j}) \;=\; \delta_{i,k}\cdot\mathbf{G}^{i,\downarrow}_U(1,V)\,\frac{1}{a} \;+\; \delta_{i,j}\cdot\mathbf{G}^{i,\uparrow}_U(1,V)\,\frac{1}{a}$$

$$\text{(G7)} \qquad \mathbf{G}^i_{\mathbf{e}_\perp^{k,j}\mathbf{e}_\perp^{k,j}}(\mathcal{E}^{k,j}) \;=\; \delta_{i,k}\cdot\mathbf{G}^{i,\downarrow}_{UU}(1,V)\,\frac{1}{a^2} \;+\; \delta_{i,j}\cdot\mathbf{G}^{i,\uparrow}_{UU}(1,V)\,\frac{1}{a^2}$$

$$\text{(G8)} \qquad \mathbf{G}^i_{\mathbf{e}_\perp^{k,j}\mathbf{e}_\parallel^{k,j}}(\mathcal{E}^{k,j}) \;=\; \delta_{i,k}\cdot\mathbf{G}^{i,\downarrow}_{UV}(1,V)\,\frac{1}{a} \;+\; \delta_{i,j}\cdot\mathbf{G}^{i,\uparrow}_{UV}(1,V)\,\frac{1}{a} \quad , \quad j=1,\dots,N \quad ,$$
$$k=(j \bmod N)+1 \quad , \quad i=j,k \quad .$$

Geometric interpretation of (H16) to (H18) and (G5) to (G8)

The geometric interpretation of conditions (H16) to (H18) and (G5) to (G8) is similar to the interpretation of the conditions for the continuity between two blending strips (see Section 4.2.2). The derivatives of the blending functions and the parameter transformations up to second order have to be equal in order to get a C^2-continuous reconstruction surface. The parameter a is a degree of freedom that we gain by linear reparameterizations. It will be used during the construction of the parameter transformations of those blending strips that are adjacent to an N-surface-blend to improve the shape of the reconstruction surface.

4.3 C^2-conditions for points where three or more patches meet

The last remaining points of the reconstruction surface we have not analyzed yet are points where three or more patches meet. Using similar charts as above, one can show that there are no further conditions for the blending functions or the parameter transformations.

5 CONSTRUCTION OF THE BLENDING FUNCTIONS

In the following we describe how to construct suitable blending functions $H^{\downarrow}$, $H^{\uparrow}$, and $H^{N,i}$ for the blending strips and the N-surface-blends. As already mentioned in Section 4, the blending functions will be constructed in a general way so that they can be applied to every blending strip or N-surface-blend of any reconstruction surface. This is appealing for practical applications because the computation of the blending functions has to be performed only once.

5.1 Construction of the blending functions of the blending strips

Besides the C^2-conditions (H1) to (H18) that we derived in Section 4 we want our blending functions $H^{\downarrow}$ and $H^{\uparrow}$ to fulfill the following conditions:

Partition of unity: Since we want our overall reconstruction method to be affine invariant, $H^{\downarrow}$ and $H^{\uparrow}$ have to fulfill

$$\text{(H19)} \qquad H^{\downarrow}(U,V) + H^{\uparrow}(U,V) \;=\; 1 \quad .$$

Reflectional symmetry in V-direction: We also want the blending strip to behave symmetrically with respect to the two B-spline-surfaces that it connects. Therefore, spatial reflection of $H^{\downarrow}$ at the axis $(U, \frac{1}{2})$, $U \in [0,1]$ has to give $H^{\uparrow}$. In other words, $H^{\downarrow}$ and $H^{\uparrow}$ have to fulfill

$$\text{(H20)} \qquad H^{\downarrow}(U,1-V) \;=\; H^{\uparrow}(U,V) \quad .$$

Translational symmetry in U-direction: Another reasonable constraint is to make the blending functions constant in U-direction,

$$\begin{aligned} \text{(H21)} \qquad H^{\downarrow}(U,V) &= H^{\downarrow}(V) \\ \text{(H22)} \qquad H^{\uparrow}(U,V) &= H^{\uparrow}(V) \quad . \end{aligned}$$

We decided to represent the blending functions as TP-Bézier-surfaces. Inserting the ansatz

$$\begin{aligned} H^{\downarrow}(U,V) &= \sum_{i=0}^{n} B_i^n(V)\, h_i^{\downarrow} \\ H^{\uparrow}(U,V) &= \sum_{i=0}^{n} B_i^n(V)\, h_i^{\uparrow} \end{aligned}$$

into the conditions (H1) to (H22) leads to a system of linear equations for the unknown control points $h_i^{\downarrow}$ and $h_i^{\uparrow}$. Note that due to (H16) this linear system is coupled with another set of linear conditions for the control points of the blending functions of the N-surface-blends. We will explain how to derive it in the next section. It turns out that $n = 7$ is the lowest degree for which a solution to the overall linear system exists. $h_i^{\downarrow}$ and $h_i^{\uparrow}$ are uniquely determined then. The numerical values of the control points are given in Appendix A.1 and the blending functions are shown in Figure 11.

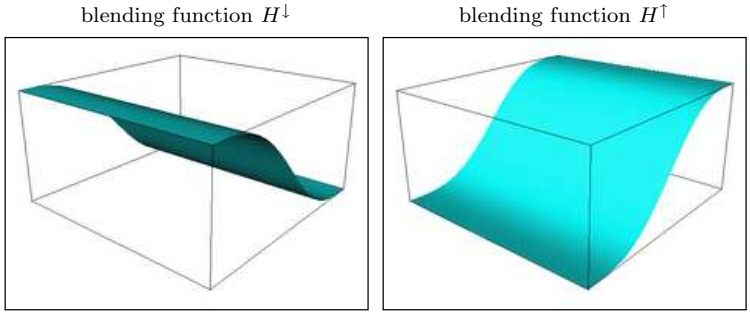

Figure 11: The blending functions $H^{\downarrow}$ and $H^{\uparrow}$ of the blending strips.

5.2 Construction of the blending functions of the N-surface-blends

Besides the C^2-conditions (H16) to (H18) that we derived in Section 4 we want our blending functions $H^{N,i}$ to fulfill the following conditions:

Partition of unity: Since we want our overall reconstruction method to be affine invariant, the blending functions $H^{N,i}$ have to fulfill

$$\text{(H23)} \qquad \sum_{i=1}^{N} H^{N,i}(U,V) \;=\; 1 \quad , \quad N = 0,1,2,\ldots \quad .$$

N-fold rotational symmetry: We also want the N-surface-blend to behave symmetrically with respect to the N B-spline-surfaces that it connects. Therefore, rotation of $H^{N,i}$ around the center of its parameter space by an angle of $\frac{2\pi}{N}$ (in the following denoted as $\mathbf{R}_{\frac{2\pi}{N}}$) has to give $H^{N,(i+1) \bmod N}$. In other words, the blending functions $H^{N,i}$ have to fulfill

$$\text{(H24)} \qquad H^{N,i}(\mathbf{R}_{\frac{2\pi}{N}}(U,V)) \;=\; H^{N,(i+1) \bmod N}(U,V) \quad , \quad i = 1,\ldots,N \quad , \quad N = 0,1,2,\ldots \quad .$$

Because of this rotational symmetry it is sufficient to compute only one of the N blending functions $H^{N,i}$. We therefore consider only $H^{N,1}$ from now on. The other $N-1$ blending functions can be generated from $H^{N,1}$ by applying the rotations $\mathbf{R}_{\frac{2\pi(i-1)}{N}}$, $i = 2,\ldots,N$.

Reflectional symmetry: A spatial reflection of the parameter space of the B-spline-surface $\mathbf{F}^i$ that corresponds to the blending function $H^{N,i}$ should not change the shape of the reconstruction surface. We accomplish this by forcing $H^{N,i}$ to have reflectional symmetry with respect to its "main axis" that is defined by the center of the parameter space and the unique corner at which $H^{N,i}$ is equal to one. Remember that this corner relates to the point where the trimmed B-spline-surface $\mathbf{F}^i$ touches the N-surface-blend. For $i = 1$ the main axis is the V-axis and we get the condition

$$\text{(H25)} \qquad H^{N,1}(1-U,V) \;=\; H^{N,1}(U,V) \quad , \quad N = 0,1,2,\ldots \quad .$$

We chose to represent the blending functions as a C^2-continuous combination of N Bézier-triangles as shown in Figure 12, i. e.,

$$
\begin{aligned}
H^{N,1} &= \bigcup_{\alpha=1}^{N} \triangle^{N,\alpha} \\
\triangle^{N,\alpha}(U,V) &= \sum_{i+j+k=n} B^n_{i,j,k}(U,V)\, h^{N,\alpha}_{i,j,k} \quad , \quad \alpha = 1,\ldots,N \quad . \qquad (12)
\end{aligned}
$$

Inserting (12) into the conditions (H16) to (H18) and (H23) to (H25) leads to a system of linear equations for the unknown control points $h^{N,\alpha}_{i,j,k}$. It is coupled to the control points of the blending functions of the blending strips due to (H16). As already mentioned, $n = 7$ is the lowest degree for which the overall system is solvable. But the control points $h^{N,\alpha}_{i,j,k}$ are not uniquely determined and we use the remaining degrees of freedom to minimize the fairness functional

$$
\mathcal{J}(H^{N,1}) = \int_{D(H^{N,1})} dU\, dV \left(\left(H^{N,1}_{UU} \right)^2 + 2 \left(H^{N,1}_{UV} \right)^2 + \left(H^{N,1}_{VV} \right)^2 \right) \quad ,
$$

that is known as the simplified thin plate energy. This functional is quadratic in the unknown control points and finding the set of admissible $h^{N,\alpha}_{i,j,k}$ that minimize it amounts to solving a linear system. The numerical values of the control points for $N = 3,\ldots,6$ are given in Appendix A.2 and three blending functions are shown in Figure 13.

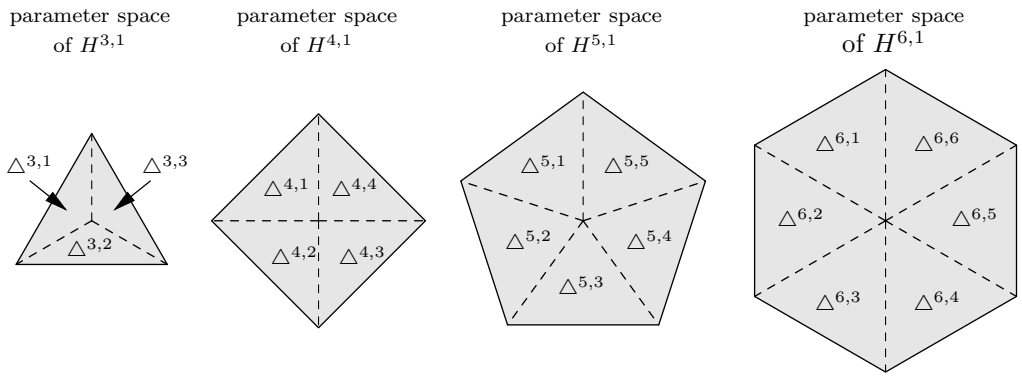

Figure 12: The partition of the parameter spaces of the blending functions $H^{N,1}$, $N = 3,\ldots,6$.

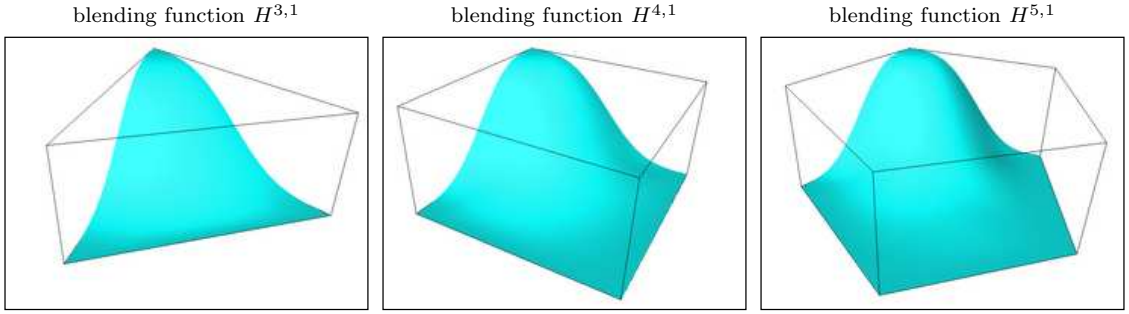

Figure 13: The blending functions $H^{3,1}$, $H^{4,1}$ and $H^{5,1}$ of the N-surface-blends.

6 CONSTRUCTION OF THE PARAMETER TRANSFORMATIONS

In this section we describe how to construct suitable parameter transformations $\mathbf{G}^{\downarrow}$, $\mathbf{G}^{\uparrow}$, and $\mathbf{G}^{i}$ for the blending strips and the N-surface-blends. Besides the C^2-conditions (G1) to (G8) that we derived in Section 4 the only other requirement for proper parameter transformations is that the resulting reconstruction surface should have a visually pleasing shape. **Since the formulation of the latter criterion is rather vague, there are numerous possible approaches to construct suitable parameter transformations.** The approach presented in this section is rather simple (we use low-degree polynomials only and all calculations and formulas have an obvious geometric meaning) but leads to good results nevertheless.

6.1 Basic Principle

We have already mentioned in Section 3.2 that we want to construct the parameter transformations such that the blending regions encompass the inverse images of those parts of the corresponding B-spline-surfaces that intersect. In other words, $\mathbf{F}$ should map the blending region approximately to that part of $\mathbb{R}^3$ where we expect the blending surface to be located. For blending strips between two B-spline-surfaces this should be close to the common boundary of the corresponding segments and for an N-surface-blend it should be near the point where the N segments meet. Therefore we construct the parameter transformations such that they define blending regions which contain the parameter values of the segment boundary points.

The size and the profile curves of the blending surfaces are determined by how far the blending regions extend to the interior and to the exterior of the corresponding segments. During the construction of the parameter transformations we use two parameters d_{in} and d_{out} that can be used to control the position and the shape of the blending regions. The parameter transformations will be constructed such that the following two conditions are fulfilled:

A) The width of the blending strips is approximately $d_{\text{in}} + d_{\text{out}}$.

B) The blending regions extend approximately $\lambda\, d_{\text{in}}$ to the interior of the corresponding segment and $\lambda\, d_{\text{out}}$ to the opposite direction (the ratio $d_{\text{in}}/d_{\text{out}}$ determines the shape of the profile curves of the blending surfaces; for more information we refer to Section 7).

After introducing a specific reparameterization in Section 6.2 that will be helpful in the subsequent sections, we describe the construction of the parameter transformations of the N-surface-blends and their adjacent blending strips in Section 6.3. These combinations of three parameter transformations will be placed near the parameter values of those vertices where three or more segments meet (vertices related to N-surface-blends). The parameter transformations of the blending strips will be used to mimic the angles of the segment boundaries at those vertices.

After the parameter transformations of all N-surface-blends and their adjacent blending strips have been calculated, we connect two of them at a time with the parameter transformations of a set of blending strips (see Section 6.4). These parameter transformations are chosen so that we get ring-like blending regions that approximate the segment boundaries respecting the two above conditions A and B.

To get a better understanding of what we are going to do, it may be beneficial to take a look at a result first. Figure 14 shows the blending region in the parameter space of one of the approximating B-spline-surfaces of the deformed tetrahedron in Figure 5. The blending region was obtained by constructing parameter transformations with the method that will be

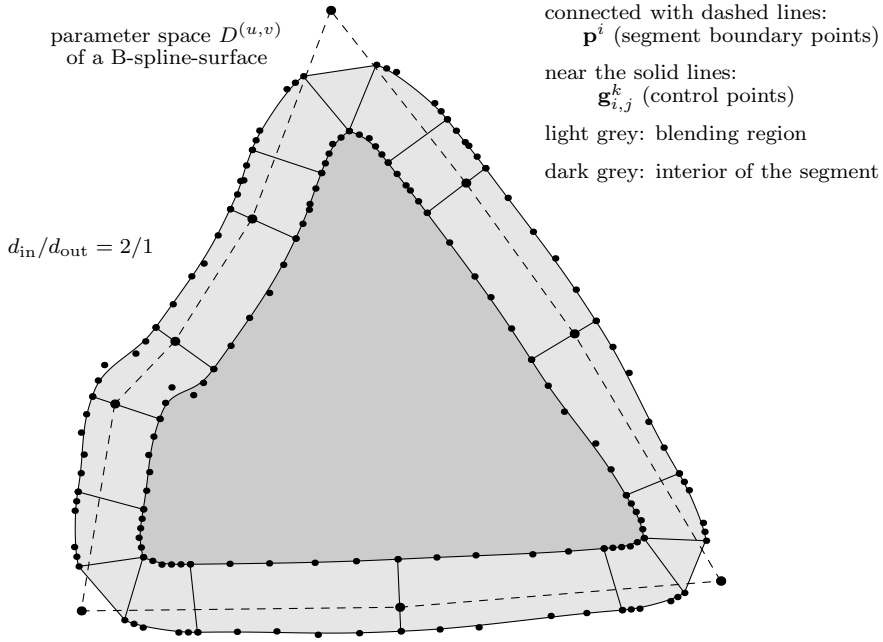

Figure 14: The blending region in the parameter space of a B-spline-surface together with the segment boundary points.

presented in the following. The blending region contains all segment boundary points (except those that relate to the N-surface-blends) and extends twice as far to the interior of the segment than to the exterior ($d_{\text{in}}/d_{\text{out}} = 2/1$ in this example). The parameter transformations of the N-surface-blends and their adjacent blending strips mimic the angles between the edges of the segment boundary at the corresponding vertices. The shape of the ring-like blending region is similar to the shape of the corresponding segment in the parameter space of the approximating B-spline-surface (the dashed line; it is given by the parameterization as explained in Section 2.2).

6.2 The reparameterizations $\mathbf{T}(u, v)$

During the construction of the parameter transformations it will often be necessary to convert angles and distances from the parameter space $D^{(u,v)}$ of a B-spline-surface $\mathbf{F}$ to three-dimensional space and vice versa. Since we are interested in a rough conversion only, we approximate the B-spline-surface near a point of interest $\mathbf{F}(u_0, v_0)$ by its tangent plane at this point and apply the reparameterization $\mathbf{T}(u_0, v_0)$ that is defined and explained below. The effect will be that angles and distances in the transformed parameter space are approximately the same as angles and distances in three-dimensional space so that no conversions are required.

For any point $(u_0, v_0) \in D^{(u,v)}$ the function $\mathbf{T}(u_0, v_0) : D^{(\tilde{u},\tilde{v})} \to D^{(u,v)}$ is an element of a set of invertible linear reparameterizations of $\mathbf{F}$, i. e.,

$$\mathbf{T}(u_0, v_0) \;=\; \begin{pmatrix} T_{1,1}(u_0, v_0) & T_{1,2}(u_0, v_0) \\ T_{2,1}(u_0, v_0) & T_{2,2}(u_0, v_0) \end{pmatrix} \quad ,$$

$$\begin{aligned} \mathbf{F}(u, v) \;&=\; \mathbf{F}(\mathbf{T}(u_0, v_0)(\tilde{u}, \tilde{v})) \;= \\ &=\; \mathbf{F}(T_{1,1}(u_0, v_0)\,\tilde{u} + T_{1,2}(u_0, v_0)\,\tilde{v}, T_{2,1}(u_0, v_0)\,\tilde{u} + T_{2,2}(u_0, v_0)\,\tilde{v})) \;=\; \tilde{\mathbf{F}}(\tilde{u}, \tilde{v}) \quad , \end{aligned}$$

such that the first fundamental form (sometimes also called metric or metric tensor) of $\tilde{\mathbf{F}}$ at (u_0, v_0) is the identity,

$$\begin{pmatrix} ((\tilde{\mathbf{F}}_{\tilde{u}}(\tilde{u}_0,\tilde{v}_0))^2 & \tilde{\mathbf{F}}_{\tilde{u}}(\tilde{u}_0,\tilde{v}_0)\tilde{\mathbf{F}}_{\tilde{v}}(\tilde{u}_0,\tilde{v}_0) \\ \tilde{\mathbf{F}}_{\tilde{u}}(\tilde{u}_0,\tilde{v}_0)\tilde{\mathbf{F}}_{\tilde{v}}(\tilde{u}_0,\tilde{v}_0) & (\tilde{\mathbf{F}}_{\tilde{v}}(\tilde{u}_0,\tilde{v}_0))^2 \end{pmatrix} = \begin{pmatrix} 1 & 0 \\ 0 & 1 \end{pmatrix} \quad . \tag{13}$$

Hence the following statements hold in the proximity of $(\tilde{u}_0, \tilde{v}_0) = (\mathbf{T}(u_0, v_0))^{-1}(u_0, v_0)$:

- Distances in the parameter space $D^{(\tilde{u},\tilde{v})}$ are approximately equal to distances in $\mathbb{R}^3$.
- Angles in the parameter space $D^{(\tilde{u},\tilde{v})}$ are approximately equal to angles in $\mathbb{R}^3$.

Of course, $\mathbf{T}(u_0, v_0)$ is not uniquely determined by (13) but a possible choice is

$$\begin{aligned} T_{1,1}(u_0,v_0) &= \pm\frac{1}{\|\mathbf{F}_u(u_0,v_0)\|} \\ T_{1,2}(u_0,v_0) &= T_{2,2}(u_0,v_0)\,\underbrace{\frac{-\mathbf{F}_u(u_0,v_0)\,\mathbf{F}_v(u_0,v_0)}{(\mathbf{F}_u(u_0,v_0))^2}}_{=C} \\ T_{2,1}(u_0,v_0) &= 0 \\ T_{2,2}(u_0,v_0) &= \pm\sqrt{\frac{1}{C^2\,(\mathbf{F}_u(u_0,v_0))^2 \,+\, 2\,C\,\mathbf{F}_u(u_0,v_0)\,\mathbf{F}_v(u_0,v_0) \,+\, (\mathbf{F}_v(u_0,v_0))^2}} \quad . \end{aligned}$$

In the following we will label functions and points in a parameter space that was generated by applying $(\mathbf{T}(u_0, v_0))^{-1}$ by the tilde symbol, e. g. $\tilde{\mathbf{G}} = (\mathbf{T}(u_0, v_0))^{-1}\mathbf{G}$ or $\tilde{\mathbf{p}} = (\mathbf{T}(u_0, v_0))^{-1}\mathbf{p}$. The reparameterizations $\mathbf{T}$ will be used whenever a simple geometric interpretation of the parameter space of a B-spline-surface is required.

6.3 The parameter transformations of an N-surface-blend and its adjacent blending strips

Let us start with the construction of the parameter transformations $\tilde{\mathbf{G}} : D^{(U,V)} \to D^{(\tilde{u},\tilde{v})}$, $\tilde{\mathbf{G}}^{\downarrow} : D^{\downarrow,(U,V)} \to D^{(\tilde{u},\tilde{v})}$, and $\tilde{\mathbf{G}}^{\uparrow} : D^{\uparrow,(U,V)} \to D^{(\tilde{u},\tilde{v})}$ of an N-surface-blend and its adjacent blending strips into the transformed parameter space $D^{(\tilde{u},\tilde{v})}$ of one of the corresponding N B-spline-surfaces (see Figure 15; reparameterization with $\mathbf{T}(\mathbf{p}^0)$ where $\mathbf{p}^0$ is the parameter value of that vertex at which the corresponding N segments meet). **We consider the parameter transformations of the N-surface-blends and their adjacent blending strips together because we want to generate a blending region that mimics the angle between the segment boundaries that meet at the vertex that relates to the N-surface-blend.**

For the parameter transformation $\tilde{\mathbf{G}}$ of the N-surface-blend we use an affine map, i. e. a combination of a rotation $\mathcal{R}$, a scaling $\mathcal{S}$, and a translation $\mathbf{t}$,

$$\tilde{\mathbf{G}}(U,V) = \begin{pmatrix} \tilde{u} \\ \tilde{v} \end{pmatrix} = \mathcal{R}\mathcal{S}\begin{pmatrix} U \\ V \end{pmatrix} + \mathbf{t} \quad . \tag{14}$$

For the parameter transformations of the blending strips $\tilde{\mathbf{G}}^{\downarrow}$ and $\tilde{\mathbf{G}}^{\uparrow}$ we use TP-Bézier-functions of degree $(5, 1)$,

$$\tilde{\mathbf{G}}^{\downarrow}(U,V) = \begin{pmatrix} \tilde{u} \\ \tilde{v} \end{pmatrix} = \sum_{i=0}^{5}\sum_{j=0}^{1} B_i^{5,[0,1]}(U)\,B_j^{1,[0,1]}(V)\,\mathbf{g}_{i,j}^{\downarrow} \tag{15}$$

$$\tilde{\mathbf{G}}^{\uparrow}(U,V) = \begin{pmatrix} \tilde{u} \\ \tilde{v} \end{pmatrix} = \sum_{i=0}^{5}\sum_{j=0}^{1} B_i^{5,[0,1]}(U)\,B_j^{1,[0,1]}(V)\,\mathbf{g}_{i,j}^{\uparrow} \quad . \tag{16}$$

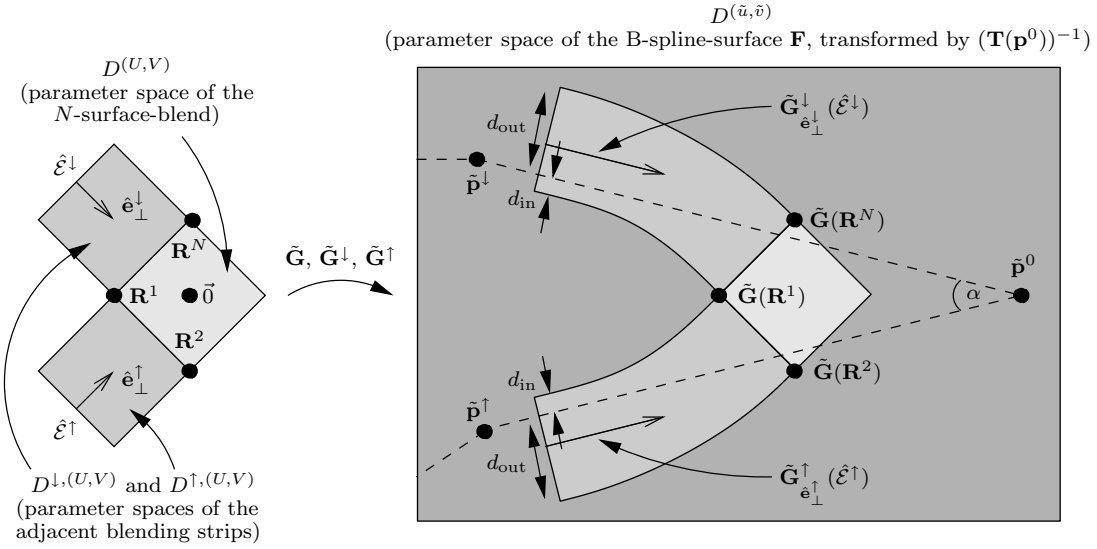

Figure 15: The parameter transformations $\tilde{\mathbf{G}}$, $\tilde{\mathbf{G}}^{\downarrow}$ and $\tilde{\mathbf{G}}^{\uparrow}$ of a 4-surface-blend and its adjacent blending-strips.

Using degree 5 in U-direction provides sufficient degrees of freedom to interpolate specific values and first and second order derivatives at both ends of the interior and the exterior boundary curves $\mathbf{G}^{\downarrow}(U,0)$, $\mathbf{G}^{\downarrow}(U,1)$, $\mathbf{G}^{\uparrow}(U,0)$, and $\mathbf{G}^{\uparrow}(U,1)$, $U \in [0,1]$.

Applying the inverse reparameterization $(\mathbf{T}(\mathbf{p}^0))^{-1}$ to the C^2-conditions (G5) to (G8) and inserting (14) and (16) leads to

$$
\begin{aligned}
\tilde{\mathbf{G}}(\mathcal{E}^{\uparrow}) &= (1-V)\,\tilde{\mathbf{G}}(\mathbf{R}^2) + V\,\tilde{\mathbf{G}}(\mathbf{R}^1) = \tilde{\mathbf{G}}^{\uparrow}(1,V) = (1-V)\,\mathbf{g}^{\uparrow}_{5,0} + V\,\mathbf{g}^{\uparrow}_{5,1} \\
\tilde{\mathbf{G}}_{\mathbf{e}_{\perp}^{\uparrow}}(\mathcal{E}^{\uparrow}) &= \mathcal{RS}\mathbf{e}_{\perp}^{\uparrow} = \tilde{\mathbf{G}}^{\uparrow}_{U}(1,V)\,\frac{1}{a} = \left((1-V)\,(\mathbf{g}^{\uparrow}_{5,0} - \mathbf{g}^{\uparrow}_{4,0}) + V\,(\mathbf{g}^{\uparrow}_{5,1} - \mathbf{g}^{\uparrow}_{4,1})\right)\frac{5}{a} \\
\tilde{\mathbf{G}}_{\mathbf{e}_{\perp}^{\uparrow}\mathbf{e}_{\perp}^{\uparrow}}(\mathcal{E}^{\uparrow}) &= 0 = \tilde{\mathbf{G}}^{\uparrow}_{UU}(1,V)\,\frac{1}{a^2} = \\
&= \left((1-V)\,(\mathbf{g}^{\uparrow}_{5,0} - 2\,\mathbf{g}^{\uparrow}_{4,0} + \mathbf{g}^{\uparrow}_{3,0}) + V\,(\mathbf{g}^{\uparrow}_{5,1} - 2\,\mathbf{g}^{\uparrow}_{4,1} + \mathbf{g}^{\uparrow}_{3,1})\right)\frac{20}{a^2} \\
\tilde{\mathbf{G}}_{\mathbf{e}_{\perp}^{\uparrow}\mathbf{e}_{\parallel}^{\uparrow}}(\mathcal{E}^{\uparrow}) &= 0 = \tilde{\mathbf{G}}^{\uparrow}_{UV}(1,V)\,\frac{1}{a} = \left(\mathbf{g}^{\uparrow}_{5,1} - \mathbf{g}^{\uparrow}_{4,1} - \mathbf{g}^{\uparrow}_{5,0} + \mathbf{g}^{\uparrow}_{4,0}\right)\frac{5}{a} \quad ,
\end{aligned}
$$

where $\mathbf{R}^1$ and $\mathbf{R}^2$ are corners of $D^{(U,V)}$ as shown in Figure 15. Simplifying these conditions yields half the unknown control points of $\tilde{\mathbf{G}}^{\uparrow}$ (see Figure 16):

$$
\begin{aligned}
\mathbf{g}^{\uparrow}_{5-i,0} &= \tilde{\mathbf{G}}(\mathbf{R}^2) - i\,\frac{a}{5}\,\mathcal{RS}\mathbf{e}_{\perp}^{\uparrow} \quad , \quad i = 0,\ldots,2 \\
\mathbf{g}^{\uparrow}_{5-i,1} &= \tilde{\mathbf{G}}(\mathbf{R}^1) - i\,\frac{a}{5}\,\mathcal{RS}\mathbf{e}_{\perp}^{\uparrow} \quad , \quad i = 0,\ldots,2 \quad .
\end{aligned}
$$

Applying the inverse reparameterization $(\mathbf{T}(\mathbf{p}^0))^{-1}$ to the C^2-conditions (G5) to (G8), inserting (14) and (15) and proceeding as above yields half of the unknown control points of $\tilde{\mathbf{G}}^{\downarrow}$ (see Figure 16):

$$
\begin{aligned}
\mathbf{g}^{\downarrow}_{5-i,0} &= \tilde{\mathbf{G}}(\mathbf{R}^1) - i\,\frac{a}{5}\,\mathcal{RS}\mathbf{e}_{\perp}^{\downarrow} \quad , \quad i = 0,\ldots,2 \\
\mathbf{g}^{\downarrow}_{5-i,1} &= \tilde{\mathbf{G}}(\mathbf{R}^N) - i\,\frac{a}{5}\,\mathcal{RS}\mathbf{e}_{\perp}^{\downarrow} \quad , \quad i = 0,\ldots,2 \quad .
\end{aligned}
$$

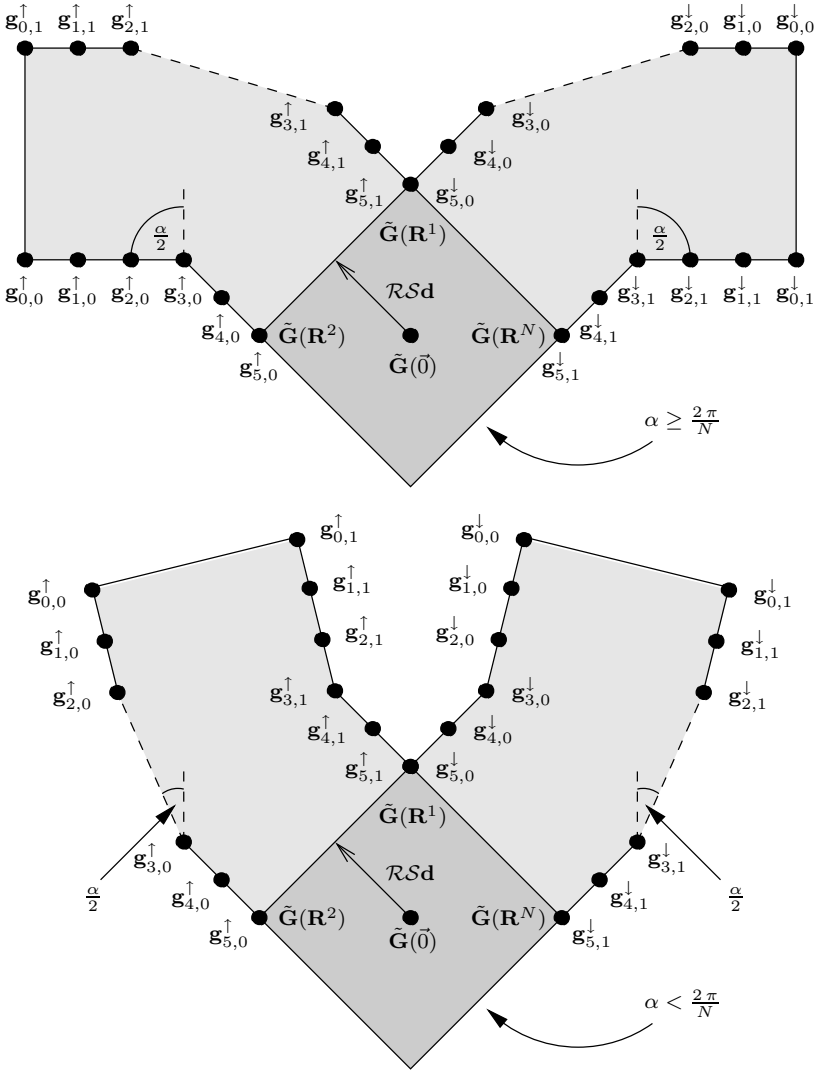

Figure 16: The positions of the control points $\mathbf{g}^{\downarrow}_{i,j}$ and $\mathbf{g}^{\uparrow}_{i,j}$ for $\alpha \geq \frac{2\pi}{N}$ and $\alpha < \frac{2\pi}{N}$.

Choosing $a = \frac{5}{2}\,\|\mathbf{d}\|$ with $\mathbf{d} = \frac{1}{2}\,(\mathbf{R}^1 + \mathbf{R}^2) - \vec{0}$ results in blending regions $\tilde{\mathbf{G}}(D^{(U,V)})$, $\tilde{\mathbf{G}}^{\downarrow}(D^{\downarrow,(U,V)})$, and $\tilde{\mathbf{G}}^{\uparrow}(D^{\uparrow,(U,V)})$ of approximately equal size.

Let $\tilde{\mathbf{p}}^0$ be the parameter value of the vertex that corresponds to the N-surface-blend, let $\tilde{\mathbf{p}}^{\downarrow}$ and $\tilde{\mathbf{p}}^{\uparrow}$ be the parameter values of the two neighbouring vertices along the segment boundary, and let α be the angle between $\tilde{\mathbf{p}}^0 - \tilde{\mathbf{p}}^{\downarrow}$ and $\tilde{\mathbf{p}}^0 - \tilde{\mathbf{p}}^{\uparrow}$. The remaining control points $\mathbf{g}^{\downarrow}_{i,j}$ and $\mathbf{g}^{\uparrow}_{i,j}$ are chosen such that the blending region $\tilde{\mathbf{G}}^{i}(D^{(U,V)}) \cup \tilde{\mathbf{G}}^{\downarrow}(D^{\downarrow,(U,V)}) \cup \tilde{\mathbf{G}}^{\uparrow}(D^{\uparrow,(U,V)})$ mimics the angle α. Or, to be more precise, the angle between the directional derivatives $\tilde{\mathbf{G}}^{\downarrow}_{\hat{\mathbf{e}}^{\downarrow}_{\perp}}(\hat{\mathcal{E}}^{\downarrow})$ and $\tilde{\mathbf{G}}^{\uparrow}_{\hat{\mathbf{e}}^{\uparrow}_{\perp}}(\hat{\mathcal{E}}^{\uparrow})$ has to be α (see Figure 15). This is achieved by choosing

$$\mathbf{g}^{\uparrow}_{i,0} \;=\; \mathbf{g}^{\uparrow}_{3,0} \,+\, (3-i)\,\frac{\|\mathbf{d}\|}{2}\,\mathcal{R}(-\sin\frac{\alpha}{2}\,,\,\cos\frac{\alpha}{2}) \quad , \quad i = 0,\ldots,2 \tag{17}$$

$$\mathbf{g}^{\uparrow}_{i,1} \;=\; \mathbf{g}^{\uparrow}_{i,0} \,+\, \mathcal{RS}(\cos\frac{\alpha}{2}\,,\,\sin\frac{\alpha}{2}) \quad , \quad i = 0,\ldots,2 \tag{18}$$

$$\mathbf{g}^{\downarrow}_{i,1} = \mathbf{g}^{\downarrow}_{3,1} + (3-i)\,\frac{\|\mathbf{d}\|}{2}\,\mathcal{R}(\sin\frac{\alpha}{2}\,,\,\cos\frac{\alpha}{2}) \quad , \quad i=0,\ldots,2 \tag{19}$$

$$\mathbf{g}^{\downarrow}_{i,0} = \mathbf{g}^{\downarrow}_{i,1} + \mathcal{R}\mathcal{S}(-\cos\frac{\alpha}{2}\,,\,\sin\frac{\alpha}{2}) \quad , \quad i=0,\ldots,2 \tag{20}$$

for angles $\alpha \geq \frac{2\pi}{N}$ (upper part of Figure 16) and choosing

$$\mathbf{g}^{\uparrow}_{i,1} = \mathbf{g}^{\uparrow}_{3,1} + (3-i)\,\frac{\|\mathbf{d}\|}{2}\,\mathcal{R}(-\sin\frac{\alpha}{2}\,,\,\cos\frac{\alpha}{2}) \quad , \quad i=0,\ldots,2 \tag{21}$$

$$\mathbf{g}^{\uparrow}_{i,0} = \mathbf{g}^{\uparrow}_{i,1} + \mathcal{R}\mathcal{S}(-\cos\frac{\alpha}{2}\,,\,-\sin\frac{\alpha}{2}) \quad , \quad i=0,\ldots,2 \tag{22}$$

$$\mathbf{g}^{\downarrow}_{i,0} = \mathbf{g}^{\downarrow}_{3,0} + (3-i)\,\frac{\|\mathbf{d}\|}{2}\,\mathcal{R}(\sin\frac{\alpha}{2}\,,\,\cos\frac{\alpha}{2}) \quad , \quad i=0,\ldots,2 \tag{23}$$

$$\mathbf{g}^{\downarrow}_{i,1} = \mathbf{g}^{\downarrow}_{i,0} + \mathcal{R}\mathcal{S}(\cos\frac{\alpha}{2}\,,\,-\sin\frac{\alpha}{2}) \quad , \quad i=0,\ldots,2 \tag{24}$$

for angles $\alpha < \frac{2\pi}{N}$ (lower part of Figure 16).

The matrices $\mathcal{R}$ and $\mathcal{S}$ and the vector $\mathbf{t}$ are determined such that the following conditions are fulfilled (see Figure 15):

- The width of the blending region is approximately $d_{\text{in}} + d_{\text{out}}$, i. e. $\|\mathbf{g}^{\downarrow}_{0,0} - \mathbf{g}^{\downarrow}_{0,1}\| = \|\mathbf{g}^{\uparrow}_{0,1} - \mathbf{g}^{\uparrow}_{0,0}\| = d_{\text{in}} + d_{\text{out}}$.
- The lines $\overline{\tilde{\mathbf{p}}^{\downarrow}\tilde{\mathbf{p}}^{0}}$ and $\overline{\tilde{\mathbf{p}}^{\uparrow}\tilde{\mathbf{p}}^{0}}$ divide the lines $\overline{\mathbf{g}^{\downarrow}_{0,0}\mathbf{g}^{\downarrow}_{0,1}}$ and $\overline{\mathbf{g}^{\uparrow}_{0,1}\mathbf{g}^{\uparrow}_{0,0}}$ at the ratio $d_{\text{in}}/d_{\text{out}}$.
- The directional derivatives $\tilde{\mathbf{G}}^{\downarrow}_{\hat{\mathbf{e}}^{\downarrow}_{\perp}}(\hat{\mathcal{E}}^{\downarrow})$ and $\tilde{\mathbf{G}}^{\uparrow}_{\hat{\mathbf{e}}^{\uparrow}_{\perp}}(\hat{\mathcal{E}}^{\uparrow})$ are parallel to $\tilde{\mathbf{p}}^{0} - \tilde{\mathbf{p}}^{\downarrow}$ and $\tilde{\mathbf{p}}^{0} - \tilde{\mathbf{p}}^{\uparrow}$.

Applying the reparameterization $\mathbf{T}(\mathbf{p}^0)$ finally leads to the parameter transformations $\mathbf{G}$, $\mathbf{G}^{\downarrow}$, and $\mathbf{G}^{\uparrow}$,

$$\mathbf{G}(U,V) = \mathbf{T}(\mathbf{p}^0)\,\tilde{\mathbf{G}}(U,V) = \mathbf{T}(\mathbf{p}^0)\,\mathcal{R}\mathcal{S}\begin{pmatrix} U \\ V \end{pmatrix} + \mathbf{T}(\mathbf{p}^0)\,\mathbf{t}$$

$$\mathbf{G}^{\downarrow}(U,V) = \mathbf{T}(\mathbf{p}^0)\,\tilde{\mathbf{G}}^{\downarrow}(U,V) = \sum_{i=0}^{5}\sum_{j=0}^{1} B_i^{5,[0,1]}(U)\,B_j^{1,[0,1]}(V)\,\mathbf{T}(\mathbf{p}^0)\,\mathbf{g}^{\downarrow}_{i,j}$$

$$\mathbf{G}^{\uparrow}(U,V) = \mathbf{T}(\mathbf{p}^0)\,\tilde{\mathbf{G}}^{\uparrow}(U,V) = \sum_{i=0}^{5}\sum_{j=0}^{1} B_i^{5,[0,1]}(U)\,B_j^{1,[0,1]}(V)\,\mathbf{T}(\mathbf{p}^0)\,\mathbf{g}^{\uparrow}_{i,j} \quad .$$

6.4 The parameter transformations of the remaining blending strips

After determining the parameter transformations of all N-surface-blends and their adjacent blending strips we connect two of them at a time with the parameter transformations of a set of blending strips so that the resulting blending regions approximate the segment boundaries.

In the following we will consider the parameter transformations of a set of blending strips between two neighbouring N-surface-blends. To keep things simple we restrict the discussion to those transformations that map the common parameter space into the parameter space of one of the two corresponding B-spline-surfaces only.

Let $\mathbf{p}^0$ and $\mathbf{p}^m$ be the parameter values of the two vertices that correspond to the two N-surface-blends that we want to connect and let $\mathbf{p}^1,\ldots,\mathbf{p}^{m-1}$ be the parameter values of the

vertices along the segment boundary between them. Further let $\mathbf{p}^{0,\text{in}}$, $\mathbf{p}^{0,\text{out}}$, $\mathbf{p}^{m,\text{in}}$, and $\mathbf{p}^{m,\text{out}}$ be the connection points that are defined by the parameter transformations of the blending strips adjacent to the N-surface blends and let $\partial\mathbf{p}^0$ and $\partial\mathbf{p}^m$ be the first directional derivatives perpendicular to the connection lines $\overline{\mathbf{p}^{0,\text{in}}\mathbf{p}^{0,\text{out}}}$ and $\overline{\mathbf{p}^{m,\text{in}}\mathbf{p}^{m,\text{out}}}$ (see Figure 17). It follows from Equations (17) to (24) that the second directional derivatives vanish, $\partial^2\mathbf{p}^0 = 0$ and $\partial^2\mathbf{p}^m = 0$. In the following we will use $\mathbf{p}^1, \ldots, \mathbf{p}^{m-1}$, $\mathbf{p}^{0,\text{in}}$, $\mathbf{p}^{0,\text{out}}$, $\mathbf{p}^{m,\text{in}}$, $\mathbf{p}^{m,\text{out}}$, $\partial\mathbf{p}^0$, $\partial\mathbf{p}^m$, $\partial^2\mathbf{p}^0$, and $\partial^2\mathbf{p}^m$ to construct the interior and the exterior boundary curves of that part of the blending region that is defined by the parameter transformations we are looking for.

The first and second derivatives of a curve that interpolates $\mathbf{p}^0, \ldots, \mathbf{p}^m$ at uniformly spaced parameter values can be estimated by finite differences (see Figure 18):

$$\partial\mathbf{p}^i = \frac{1}{2}\left(\mathbf{p}^{i+1} - \mathbf{p}^{i-1}\right) \quad , \quad i = 1, \ldots, m-1 \tag{25}$$

$$\partial^2\mathbf{p}^i = \mathbf{p}^{i+1} - 2\,\mathbf{p}^i + \mathbf{p}^{i-1} \quad , \quad i = 1, \ldots, m-1 \quad . \tag{26}$$

We use the first derivatives $\partial\mathbf{p}^i$ to compute interpolation points $\mathbf{p}^{i,\text{in}}$ and $\mathbf{p}^{i,\text{out}}$, $i = 1, \ldots, m-1$ for the interior and exterior boundary curves of the blending region in the following way. Let $\tilde{\mathbf{p}}^i = (\mathbf{T}(\mathbf{p}^i))^{-1}\,\mathbf{p}^i$, $\tilde{\mathbf{p}}^{i,\text{in}} = (\mathbf{T}(\mathbf{p}^i))^{-1}\,\mathbf{p}^{i,\text{in}}$, $\tilde{\mathbf{p}}^{i,\text{out}} = (\mathbf{T}(\mathbf{p}^i))^{-1}\,\mathbf{p}^{i,\text{out}}$, and $\partial\tilde{\mathbf{p}}^i = (\mathbf{T}(\mathbf{p}^i))^{-1}\,\partial\mathbf{p}^i$. Then the interpolation points $\mathbf{p}^{i,\text{in}}$ and $\mathbf{p}^{i,\text{out}}$ are specified such that the vectors $\tilde{\mathbf{p}}^{i,\text{in}} - \tilde{\mathbf{p}}^i$ and $\tilde{\mathbf{p}}^{i,\text{out}} - \tilde{\mathbf{p}}^i$ are perpendicular to the transformed first derivatives $\partial\tilde{\mathbf{p}}^i$ and have length d_{in} and d_{out}, respectively (see Figure 18).

In order to construct parameter transformations that interpolate the points $\mathbf{p}^{i,\text{in}}$ and $\mathbf{p}^{i,\text{out}}$, $i = 0, \ldots, m$ with their interior and exterior boundary curves we use m TP-Bézier-functions of degree $(5, 1)$,

$$\mathbf{G}^k(U,V) = \begin{pmatrix} u \\ v \end{pmatrix} = \sum_{i=0}^{5}\sum_{j=0}^{1} B_i^{5,[0,1]}(U)\,B_j^{1,[0,1]}(V)\,\mathbf{g}_{i,j}^k \quad , \quad k = 1, \ldots, m \quad , \tag{27}$$

and choose $\mathbf{g}_{0,0}^k = \mathbf{p}^{k-1,\text{out}}$, $\mathbf{g}_{0,1}^k = \mathbf{p}^{k-1,\text{in}}$, $\mathbf{g}_{5,0}^k = \mathbf{p}^{k,\text{out}}$, and $\mathbf{g}_{5,1}^k = \mathbf{p}^{k,\text{in}}$. Note that condition (G1) is met automatically this way. As already mentioned above, using degree 5 in U-direction enables us to interpolate given values and given first and second derivatives at both ends of the interior and exterior boundary curves.

We further want the directions of the first derivatives $\mathbf{G}_U^k(0,V)$ and $\mathbf{G}_U^k(1,V)$ at the connection lines $(0,V)$ and $(1,V)$, $V \in [0,1]$ to be equal to the directions of the estimated first

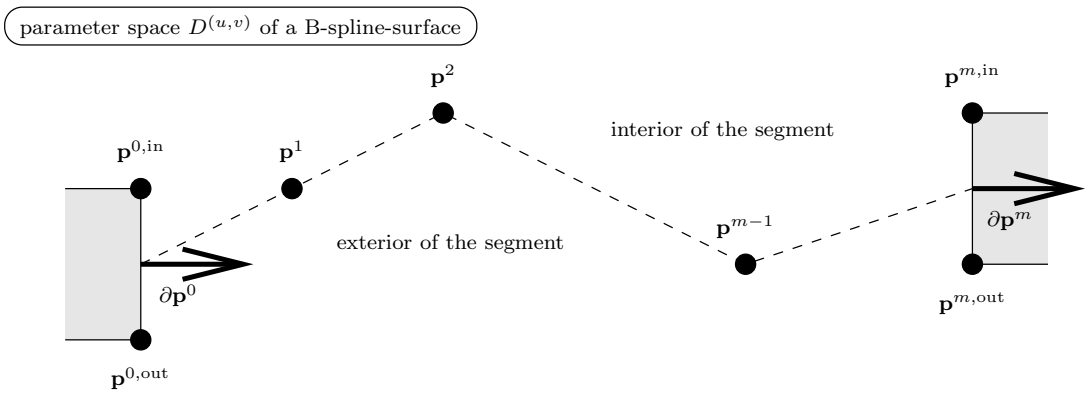

Figure 17: A segment boundary that has to be covered with blending strip transformations.

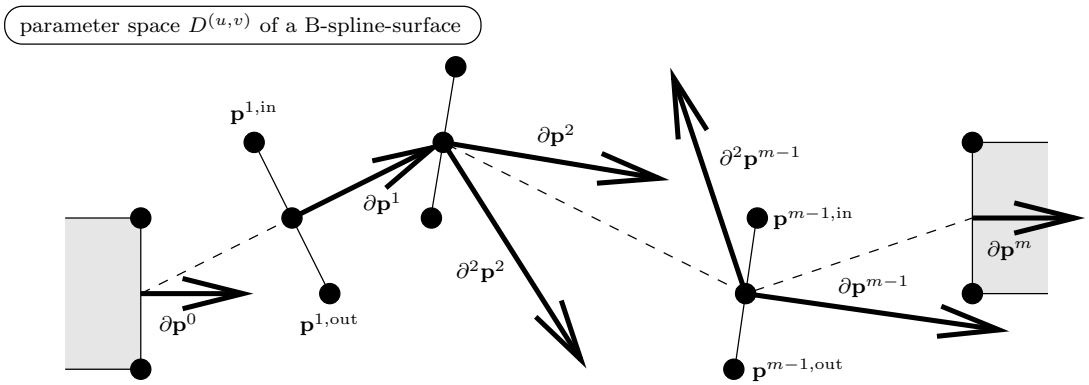

Figure 18: Estimated first and second derivatives and interpolation points for the interior and exterior boundary curves.

derivatives $\partial\mathbf{p}^{k-1}$ and $\partial\mathbf{p}^k$, respectively. In order to place the remaining control points approximately equidistantly (this will lead to boundary curves of smooth shape) we choose

$$\mathbf{g}^k_{1,j} = \mathbf{g}^k_{0,j} + \frac{\|\mathbf{p}^k - \mathbf{p}^{k-1}\|}{5} \frac{\partial\mathbf{p}^{k-1}}{\|\partial\mathbf{p}^{k-1}\|} \quad , \quad j = 0,1 \quad , \quad k = 1,\ldots,m \tag{28}$$

$$\mathbf{g}^k_{4,j} = \mathbf{g}^k_{5,j} - \frac{\|\mathbf{p}^k - \mathbf{p}^{k-1}\|}{5} \frac{\partial\mathbf{p}^{k}}{\|\partial\mathbf{p}^{k}\|} \quad , \quad j = 0,1 \quad , \quad k = 1,\ldots,m \quad . \tag{29}$$

The conditions (G2) and (G4) are thus fulfilled and we can use Equations (27), (28), and (29) to compute the unknown factors a and $\tilde{a}$:

$$\mathbf{G}^k_U(0,V) = \underbrace{\frac{\|\mathbf{p}^k - \mathbf{p}^{k-1}\|}{\|\partial\mathbf{p}^{k-1}\|}}_{=\tilde{a}_k} \partial\mathbf{p}^{k-1} \quad , \quad k = 1,\ldots,m \tag{30}$$

$$\mathbf{G}^k_U(1,V) = \underbrace{\frac{\|\mathbf{p}^k - \mathbf{p}^{k-1}\|}{\|\partial\mathbf{p}^{k}\|}}_{=a_k} \partial\mathbf{p}^{k} \quad , \quad k = 1,\ldots,m \quad . \tag{31}$$

Until now we have considered the mappings into the parameter space of one of the two B-spline-surfaces only. But to make sure that the conditions (G2) to (G4) are fulfilled we have to take both mappings into account. Since the parameter space of every blending strip is mapped to the parameter spaces of two different B-spline-surfaces (indexed with $\downarrow$ and $\uparrow$ in (G2) to (G4)), Equations (30) and (31) yield two different, although usually very similar values $\tilde{a}^{\downarrow}_k$ and $\tilde{a}^{\uparrow}_k$ for $\tilde{a}_k$, and $a^{\downarrow}_k$ and $a^{\uparrow}_k$ for a_k, thus violating conditions (G2) to (G4). To overcome this drawback we compute the averages $\overline{\tilde{a}}_k = \frac{1}{2}(\tilde{a}^{\downarrow}_k + \tilde{a}^{\uparrow}_k)$ and $\overline{a}_k = \frac{1}{2}(a^{\downarrow}_k + a^{\uparrow}_k)$ of the two values for $\tilde{a}_k$ and a_k and recalculate the control points $\mathbf{g}^k_{1,j},\ldots,\mathbf{g}^k_{4,j}$ using (G2) to (G4) and Equation (27):

$$\mathbf{g}^k_{1,j} = \mathbf{g}^k_{0,j} + \frac{\overline{\tilde{a}}_k}{5} \partial\mathbf{p}^{k-1} \quad , \quad j = 0,1 \quad , \quad k = 1,\ldots,m$$

$$\mathbf{g}^k_{4,j} = \mathbf{g}^k_{5,j} - \frac{\overline{a}_k}{5} \partial\mathbf{p}^{k} \quad , \quad j = 0,1 \quad , \quad k = 1,\ldots,m$$

$$\mathbf{g}^k_{2,j} = -\mathbf{g}^k_{0,j} + 2\,\mathbf{g}^k_{1,j} + \frac{(\overline{\tilde{a}}_k)^2}{20} \partial^2\mathbf{p}^{k-1} \quad , \quad j = 0,1 \quad , \quad k = 1,\ldots,m$$

$$\mathbf{g}^k_{3,j} \;=\; -\mathbf{g}^k_{5,j} \,+\, 2\,\mathbf{g}^k_{4,j} \,+\, \frac{(\overline{a}_k)^2}{20}\,\partial^2\mathbf{p}^k \quad , \quad j = 0,1 \quad , \quad k = 1,\ldots,m \quad .$$

By doing so we preserve the shape of the blending regions (the boundary curves will not change significantly) and we assure the C^2-continuity of the reconstruction surface.

We would like to mention that the resulting reconstruction surface will not be C^2-continuous if the blending regions that are defined by the parameter transformations of the blending strips and the N-surface-blends have any self-intersections. In that case, the user has to choose a smaller blending region, i. e. other values for d_{in} and d_{out} or create a different segmentation.

Remark on using using TP-B-spline-functions instead of TP-Bézier-functions

A more elegant way to express the parameter transformations for a set of blending strips that connect two neighbouring N-surface-blends is to use a single TP-B-spline-function instead of many TP-Bézier-functions. Nevertheless we decided to work with the Bézier-form since the geometric interpretation of the control points is more intuitive for Bézier-functions than for B-spline-functions.

Of course both representations are equivalent and we can convert the $m+2$ C^2-continuously connected Bézier-functions of degree $(5,1)$ to a single B-spline-function of degree $(5,1)$ with a knot vector in U-direction defined by the values $\overline{\overline{a}}_k$ and $\overline{a}_k$, respectively. To reduce the continuity from C^4 to C^2 (otherwise there would not be sufficient degrees of freedom to interpolate the estimated first and second derivatives $\partial\mathbf{p}^k$ and $\partial^2\mathbf{p}^k$) every knot must have a multiplicity of 3. The control points of the B-spline-function can be found by solving a linear system.

6.5 Extensions

To further improve the quality of the reconstruction surface the following steps can be taken.

Ignoring segment boundary points: With the method presented in Section 6.4 we construct approximately as many blending strips as there are segment boundary points. If the average distance between two segment boundary points is significantly less than the approximate width $d_{\text{in}} + d_{\text{out}}$ of the blending strips we get unnecessarily many blending strips, often leading to an unnatural shape. To prevent that we ignore as many segment boundary points so that no two adjacent points are closer than the user defined parameter d_{min}. Choosing $d_{\text{min}} = d_{\text{in}} + d_{\text{out}}$ gives good results in most cases.

Correcting the parameter values of the segment boundary points: To improve the visual smoothness of the blending strip that connects two B-spline-surfaces we change the parameter values of the segment boundary points before computing the parameter transformations. Every parameter value is moved in the direction of its estimated second derivative $\partial^2\mathbf{p}^i$ (see Equation (26)), i. e., $\mathbf{p}^i \rightarrow \mathbf{p}^i + d_{\partial^2}\,\partial^2\mathbf{p}^i$. We found $d_{\partial^2} = 0.3$ to give good results in most cases.

7 RESULTS AND CONCLUSION

We presented a new method to generate reconstruction surfaces from arbitrary manifold triangle meshes. The reconstruction surfaces have the following properties:

- The reconstruction surfaces are C^2-continuous everywhere and watertight, i. e., the C^2-continuity is of mathematical and not only of numerical exactness.
- The number of patches that form the reconstruction surface does not dependent on the number of triangles in the input triangulation. For a big input triangle mesh the number of patches is therefore significantly smaller than the number of triangles.
- All patches are compositions of low-degree-polynomials. Therefore storage and evaluation of these patches are both very efficient.

Figures 20 to 22 show several input triangle meshes and the corresponding reconstruction surfaces both uniformly coloured so as to see the visual smoothness and coloured in accordance with the patch type in order to show the structure of the reconstruction surface (yellow: N-surface-blends; green: blending strips that are adjacent to N-surface-blends; red and light-red: all other blending strips; blue: trimmed B-spline-surfaces).

The user-defined parameters d_{in} and d_{out} are related to shape control. The reconstruction surface is constructed so that the width of the blending strips is approximately $d_{\text{in}} + d_{\text{out}}$. The ratio $d_{\text{in}}/d_{\text{out}}$ controls the profile curves of the blending surfaces. Choosing $d_{\text{in}}/d_{\text{out}} \approx 2/1$ leads to good results in most cases. Figure 19 shows the effect of choosing different values for d_{in} and d_{out}.

Our method is currently limited to manifold triangle meshes, i. e. closed surfaces with arbitrary genus. But the ideas and principles that we present in this report are not applicable to closed surfaces only. Future work should lead to similar techniques that will be able to handle boundaries as well.

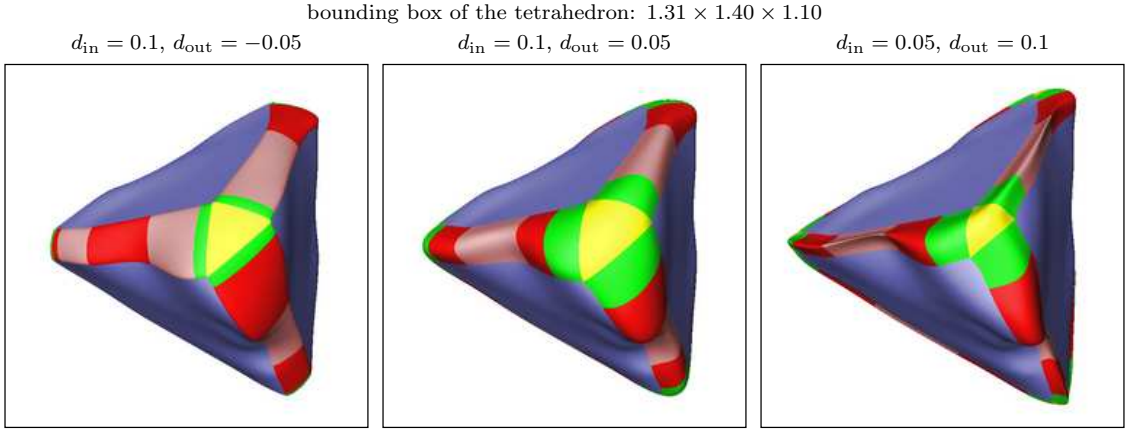

Figure 19: Reconstruction of a deformed tetrahedron with different values for d_{in} and d_{out}.

deformed tetrahedron (196 triangles, 4 segments, 4 N-surface-blends, 24 blending stripes)

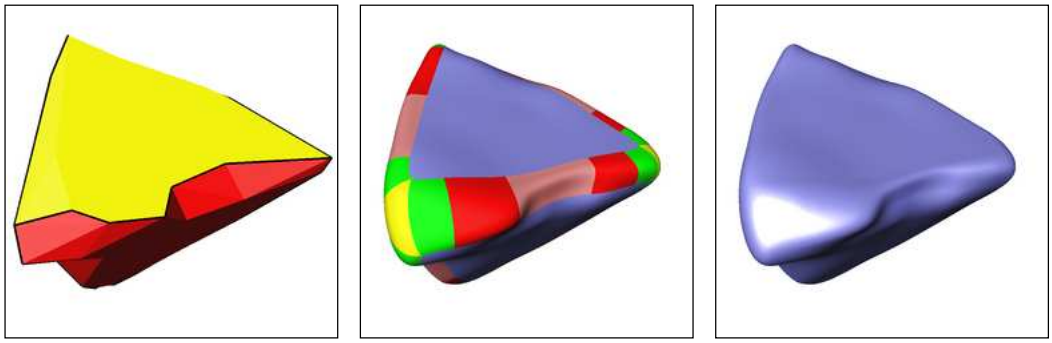

sphere (320 triangles, 5 segments, 6 N-surface-blends, 52 blending stripes)

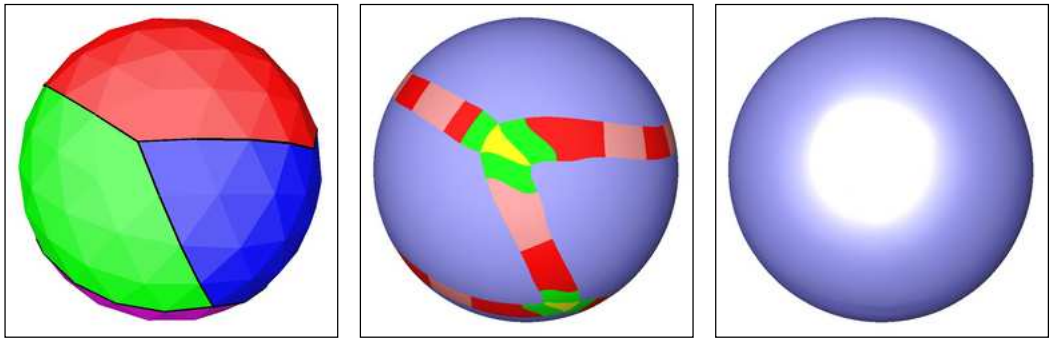

L-shape (448 triangles, 12 segments, 16 N-surface-blends, 126 blending stripes)

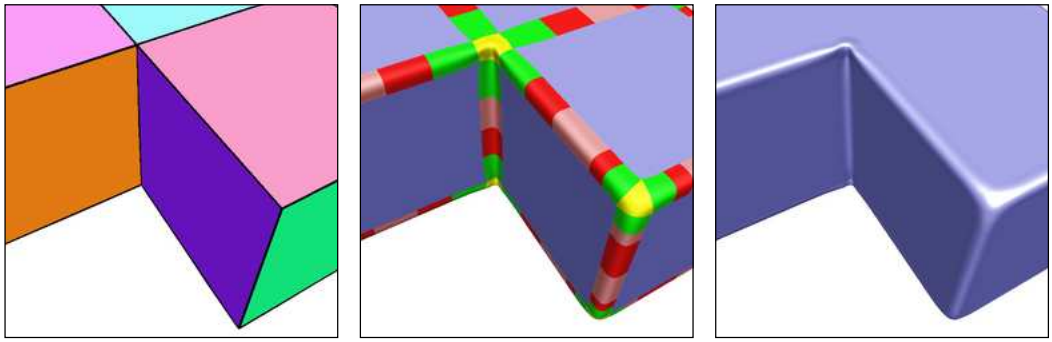

torus (2304 triangles, 8 segments, 8 N-surface-blends, 152 blending stripes)

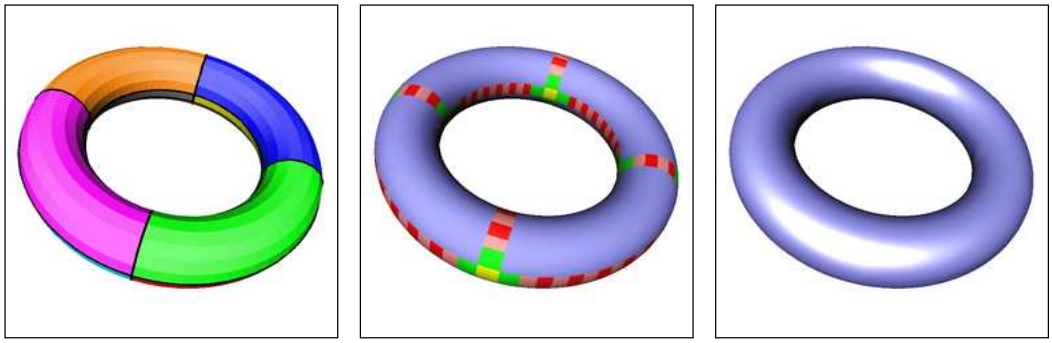

Figure 20: Watertight C^2-continuous reconstruction surfaces.

deformed octahedron (128 triangles, 8 segments, 6 N-surface-blends, 53 blending stripes)

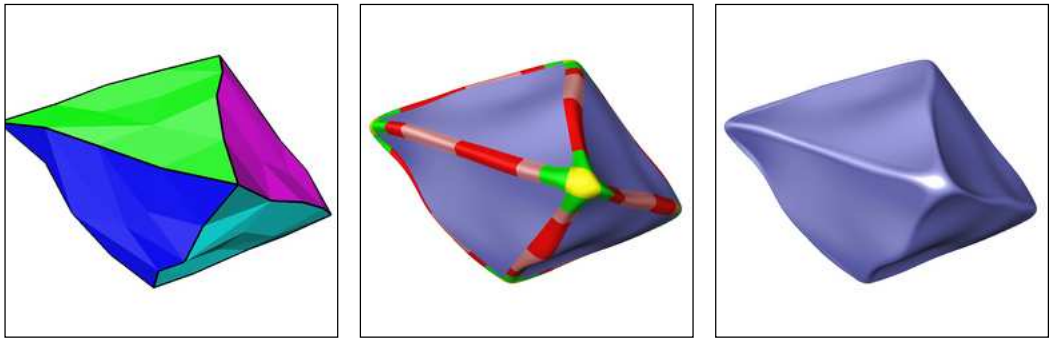

cylinder (2736 triangles, 6 segments, 8 N-surface-blends, 132 blending stripes)

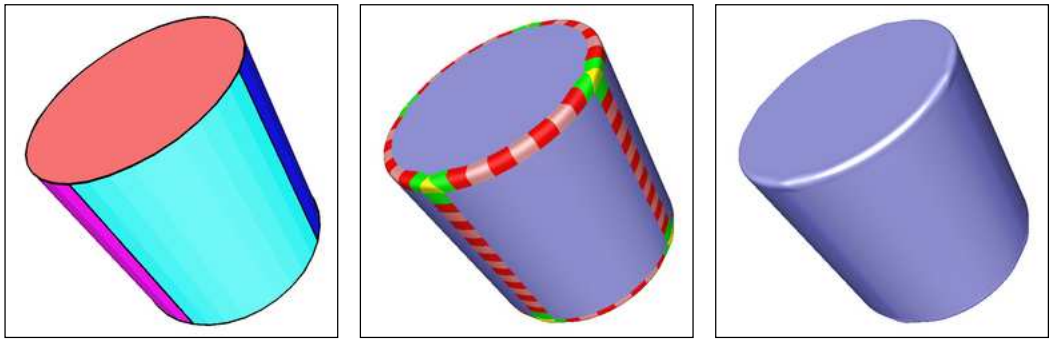

fandisk (12946 triangles, 20 segments, 32 N-surface-blends, 857 blending stripes)

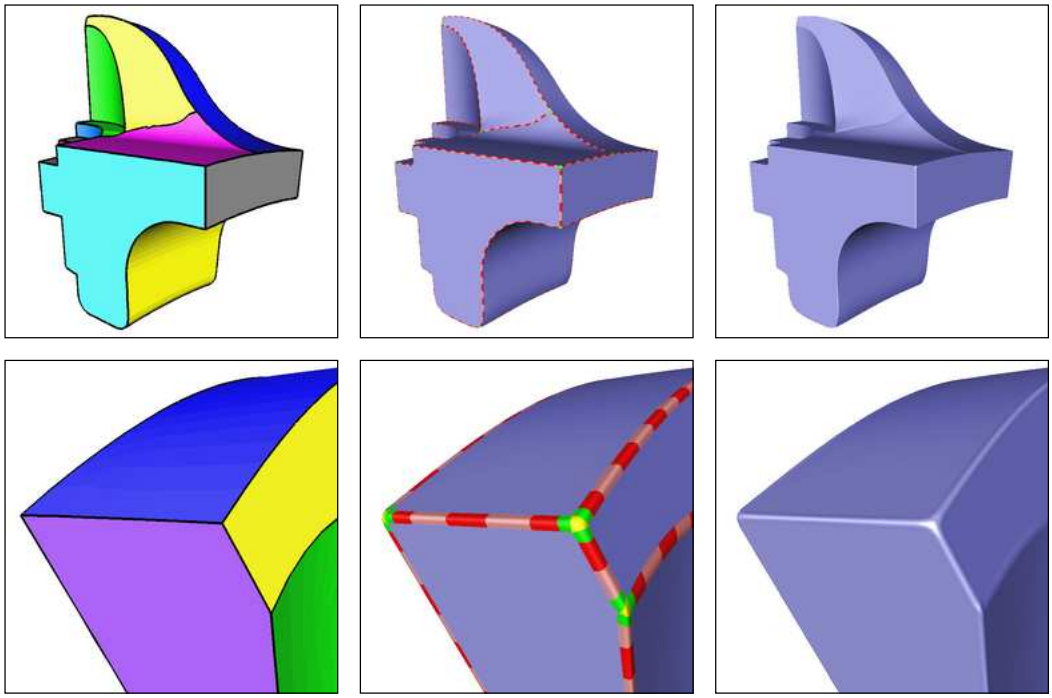

Figure 21: Watertight C^2-continuous reconstruction surfaces.

cat (728 triangles, 4 segments, 4 N-surface-blends, 58 blending stripes)

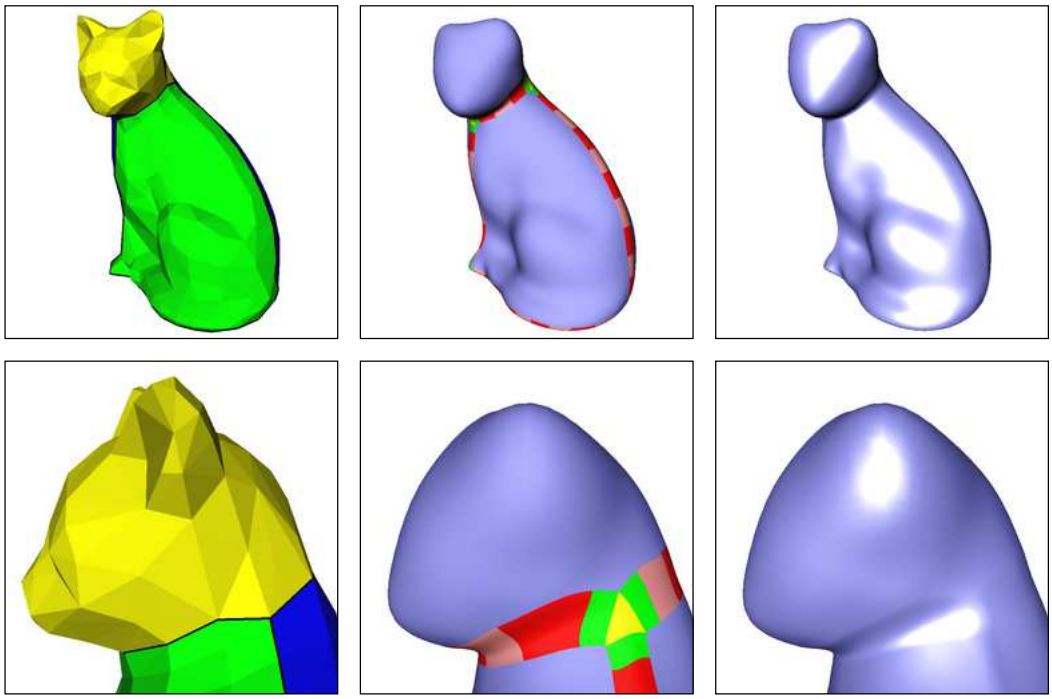

cat (728 triangles, 9 segments, 11 N-surface-blends, 139 blending stripes)

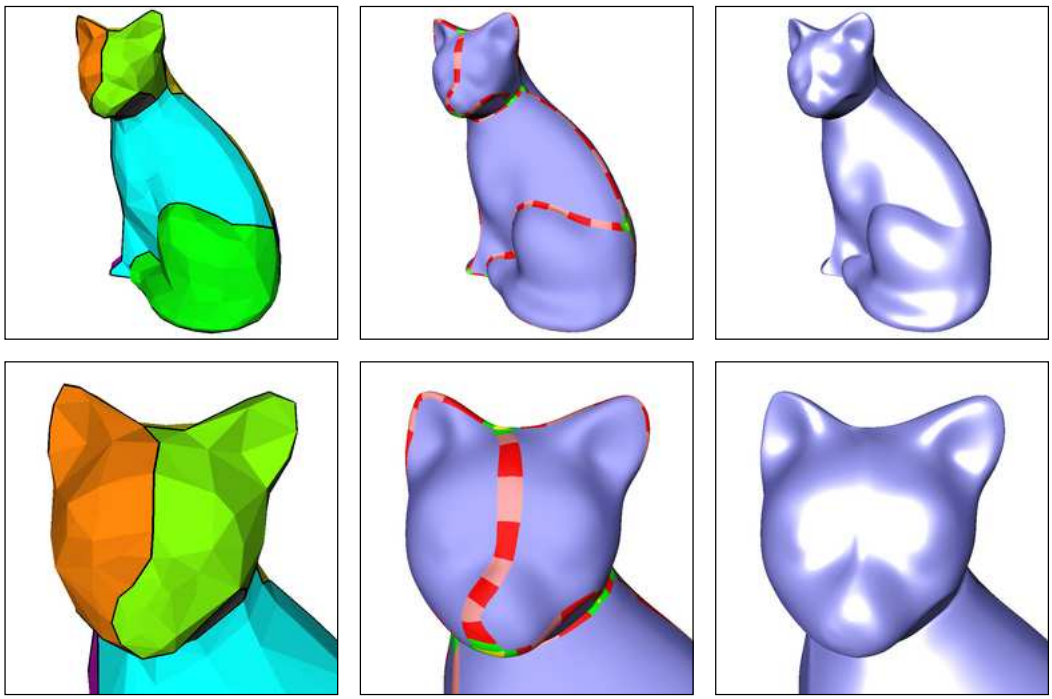

Figure 22: Watertight C^2-continuous reconstruction surfaces.

A THE CONTROL POINTS OF THE BLENDING FUNCTIONS

In the following we give the numerical values of the control points of the blending functions.

A.1 The control points of the blending functions of the blending strips

The blending functions $H^{\downarrow}$ and $H^{\uparrow}$ of the blending strips are TP-Bézier-patches of degree $(0,7)$ (see Section 5.1),

$$\begin{aligned} H^{\downarrow}(U,V) &= \sum_{i=0}^{7} B_i^7(V)\, h_i^{\downarrow} \\ H^{\uparrow}(U,V) &= \sum_{i=0}^{7} B_i^7(V)\, h_i^{\uparrow} \end{aligned}$$

and the control points $h_i^{\downarrow}$ and $h_i^{\uparrow}$ are

$$\begin{aligned} h_i^{\downarrow} &= h_{7-i}^{\uparrow} = 1 \quad , \quad i = 0,\ldots,3 \\ h_i^{\downarrow} &= h_{7-i}^{\uparrow} = 0 \quad , \quad i = 4,\ldots,7 \quad . \end{aligned}$$

A.2 The control points of the blending functions of the N-surface-blends

The blending functions $H^{N,1}$ of the N-surface-blends are C^2-continuous combinations of N Bézier-triangles of degree 7 (see Section 5.2),

$$\begin{aligned} H^{N,1} &= \bigcup_{\alpha=1}^{N} \triangle^{N,\alpha} \\ \triangle^{N,\alpha}(U,V) &= \sum_{i+j+k=7} B_{i,j,k}^7(U,V)\, h_{i,j,k}^{N,\alpha} \quad , \quad \alpha = 1,\ldots,N \quad . \end{aligned}$$

The relation between the indices i, j, k and α and the positions of the control points $h_{i,j,k}^{N,\alpha}$ are shown in Figure 23. The blending functions $H^{N,i}$, $i = 2,\ldots,N$, and their control points can be obtained by applying the rotations $\mathbf{R}_{\frac{2\pi(i-1)}{N}}$ (see Section 5.2).

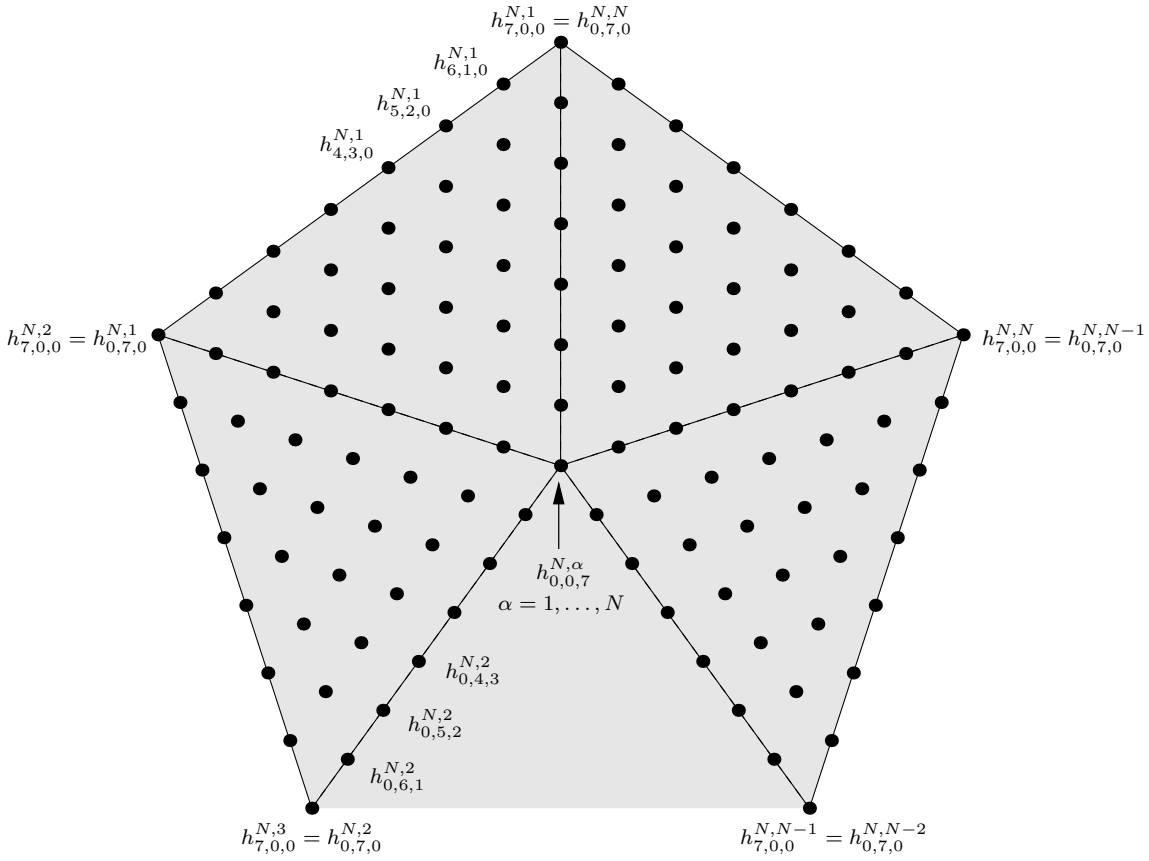

Figure 23: The positions of the control points $h^{N,\alpha}_{i,j,k}$.

A.2.1 The numerical values of the control points of $H^{3,1}$

$\triangle^{3,1}$		
Control points $h^{3,1}_{i,j,k}$ with $h^{3,1}_{i,j,k} = 0$: $h^{3,1}_{0,4,3}$, $h^{3,1}_{0,5,2}$, $h^{3,1}_{0,6,1}$, $h^{3,1}_{0,7,0}$, $h^{3,1}_{1,4,2}$, $h^{3,1}_{1,5,1}$, $h^{3,1}_{1,6,0}$, $h^{3,1}_{2,4,1}$, $h^{3,1}_{2,5,0}$, $h^{3,1}_{3,4,0}$		
Control points $h^{3,1}_{i,j,k}$ with $h^{3,1}_{i,j,k} = 1$: $h^{3,1}_{4,0,3}$, $h^{3,1}_{4,1,2}$, $h^{3,1}_{4,2,1}$, $h^{3,1}_{4,3,0}$, $h^{3,1}_{5,0,2}$, $h^{3,1}_{5,1,1}$, $h^{3,1}_{5,2,0}$, $h^{3,1}_{6,0,1}$, $h^{3,1}_{6,1,0}$, $h^{3,1}_{7,0,0}$		
Remaining control points $h^{3,1}_{i,j,k}$:		
$h^{3,1}_{0,0,7} = 0.3333333333$	$h^{3,1}_{0,1,6} = 0.2486889093$	$h^{3,1}_{0,2,5} = 0.1503469034$
$h^{3,1}_{0,3,4} = 0.0657943067$	$h^{3,1}_{1,0,6} = 0.5026221814$	$h^{3,1}_{1,1,5} = 0.4042801755$
$h^{3,1}_{1,2,4} = 0.2647535966$	$h^{3,1}_{1,3,3} = 0.1403581267$	$h^{3,1}_{2,0,5} = 0.6993061932$
$h^{3,1}_{2,1,4} = 0.6147535966$	$h^{3,1}_{2,2,3} = 0.4498163453$	$h^{3,1}_{2,3,2} = 0.2500000000$
$h^{3,1}_{3,0,4} = 0.8684113866$	$h^{3,1}_{3,1,3} = 0.8026170799$	$h^{3,1}_{3,2,2} = 0.7500000000$
$h^{3,1}_{3,3,1} = 0.5000000000$		

$\triangle^{3,2}$		
Control points $h^{3,2}_{i,j,k}$ with $h^{3,2}_{i,j,k} = 0$:		
$h^{3,2}_{0,4,3}$, $h^{3,2}_{0,5,2}$, $h^{3,2}_{0,6,1}$, $h^{3,2}_{0,7,0}$, $h^{3,2}_{1,4,2}$, $h^{3,2}_{1,5,1}$, $h^{3,2}_{1,6,0}$, $h^{3,2}_{2,3,2}$, $h^{3,2}_{2,4,1}$, $h^{3,2}_{2,5,0}$, $h^{3,2}_{3,2,2}$, $h^{3,2}_{3,3,1}$, $h^{3,2}_{3,4,0}$, $h^{3,2}_{4,0,3}$, $h^{3,2}_{4,1,2}$, $h^{3,2}_{4,2,1}$, $h^{3,2}_{4,3,0}$, $h^{3,2}_{5,0,2}$, $h^{3,2}_{5,1,1}$, $h^{3,2}_{5,2,0}$, $h^{3,2}_{6,0,1}$, $h^{3,2}_{6,1,0}$, $h^{3,2}_{7,0,0}$		
Remaining control points $h^{3,2}_{i,j,k}$:		
$h^{3,2}_{0,0,7} = 0.3333333333$	$h^{3,2}_{0,1,6} = 0.2486889093$	$h^{3,2}_{0,2,5} = 0.1503469034$
$h^{3,2}_{0,3,4} = 0.0657943067$	$h^{3,2}_{1,0,6} = 0.2486889093$	$h^{3,2}_{1,1,5} = 0.1914396490$
$h^{3,2}_{1,2,4} = 0.1204928069$	$h^{3,2}_{1,3,3} = 0.0570247934$	$h^{3,2}_{2,0,5} = 0.1503469034$
$h^{3,2}_{2,1,4} = 0.1204928069$	$h^{3,2}_{2,2,3} = 0.1003673095$	$h^{3,2}_{3,0,4} = 0.0657943067$
$h^{3,2}_{3,1,3} = 0.0570247934$		

Because of the reflectional symmetry of the blending functions of the N-surface-blends (H25) the control points of the Bézier-triangle $\triangle^{3,3}$ are given by

$$h^{3,3}_{i,j,k} \quad = \quad h^{3,1}_{j,i,k} \quad .$$

A.2.2 The numerical values of the control points of $H^{4,1}$

$\triangle^{4,1}$		
Control points $h^{4,1}_{i,j,k}$ with $h^{4,1}_{i,j,k} = 0$:		
$h^{4,1}_{0,4,3}$, $h^{4,1}_{0,5,2}$, $h^{4,1}_{0,6,1}$, $h^{4,1}_{0,7,0}$, $h^{4,1}_{1,4,2}$, $h^{4,1}_{1,5,1}$, $h^{4,1}_{1,6,0}$, $h^{4,1}_{2,4,1}$, $h^{4,1}_{2,5,0}$, $h^{4,1}_{3,4,0}$		
Control points $h^{4,1}_{i,j,k}$ with $h^{4,1}_{i,j,k} = 1$:		
$h^{4,1}_{4,0,3}$, $h^{4,1}_{4,1,2}$, $h^{4,1}_{4,2,1}$, $h^{4,1}_{4,3,0}$, $h^{4,1}_{5,0,2}$, $h^{4,1}_{5,1,1}$, $h^{4,1}_{5,2,0}$, $h^{4,1}_{6,0,1}$, $h^{4,1}_{6,1,0}$, $h^{4,1}_{7,0,0}$		
Remaining control points $h^{4,1}_{i,j,k}$:		
$h^{4,1}_{0,0,7} = 0.2500000000$	$h^{4,1}_{0,1,6} = 0.2500000000$	$h^{4,1}_{0,2,5} = 0.1962068966$
$h^{4,1}_{0,3,4} = 0.1700000000$	$h^{4,1}_{1,0,6} = 0.3737091222$	$h^{4,1}_{1,1,5} = 0.3737091222$
$h^{4,1}_{1,2,4} = 0.2948425104$	$h^{4,1}_{1,3,3} = 0.2325000000$	$h^{4,1}_{2,0,5} = 0.5512113479$
$h^{4,1}_{2,1,4} = 0.5512113479$	$h^{4,1}_{2,2,3} = 0.4472712278$	$h^{4,1}_{2,3,2} = 0.2500000000$
$h^{4,1}_{3,0,4} = 0.6586090792$	$h^{4,1}_{3,1,3} = 0.6586090792$	$h^{4,1}_{3,2,2} = 0.7500000000$
$h^{4,1}_{3,3,1} = 0.5000000000$		

$\triangle^{4,2}$
Control points $h^{4,2}_{i,j,k}$ with $h^{4,2}_{i,j,k} = 0$: $h^{4,2}_{0,4,3}$, $h^{4,2}_{0,5,2}$, $h^{4,2}_{0,6,1}$, $h^{4,2}_{0,7,0}$, $h^{4,2}_{1,4,2}$, $h^{4,2}_{1,5,1}$, $h^{4,2}_{1,6,0}$, $h^{4,2}_{2,3,2}$, $h^{4,2}_{2,4,1}$, $h^{4,2}_{2,5,0}$, $h^{4,2}_{3,2,2}$, $h^{4,2}_{3,3,1}$, $h^{4,2}_{3,4,0}$, $h^{4,2}_{4,0,3}$, $h^{4,2}_{4,1,2}$, $h^{4,2}_{4,2,1}$, $h^{4,2}_{4,3,0}$, $h^{4,2}_{5,0,2}$, $h^{4,2}_{5,1,1}$, $h^{4,2}_{5,2,0}$, $h^{4,2}_{6,0,1}$, $h^{4,2}_{6,1,0}$, $h^{4,2}_{7,0,0}$
Remaining control points $h^{4,2}_{i,j,k}$: $h^{4,2}_{0,0,7} = 0.2500000000$ $h^{4,2}_{0,1,6} = 0.1262908778$ $h^{4,2}_{0,2,5} = 0.0563748590$ $h^{4,2}_{0,3,4} = 0.0013909208$ $h^{4,2}_{1,0,6} = 0.2500000000$ $h^{4,2}_{1,1,5} = 0.1262908778$ $h^{4,2}_{1,2,4} = 0.0563748590$ $h^{4,2}_{1,3,3} = 0.0013909208$ $h^{4,2}_{2,0,5} = 0.1962068966$ $h^{4,2}_{2,1,4} = 0.0975712827$ $h^{4,2}_{2,2,3} = 0.0527287722$ $h^{4,2}_{3,0,4} = 0.1700000000$ $h^{4,2}_{3,1,3} = 0.1075000000$

Because of the reflectional symmetry of the blending functions of the N-surface-blends (H25) the control points of the Bézier-triangles $\triangle^{4,3}$ and $\triangle^{4,4}$ are given by

$$\begin{aligned} h^{4,3}_{i,j,k} &= h^{4,2}_{j,i,k} \\ h^{4,3}_{i,j,k} &= h^{4,1}_{j,i,k} \quad . \end{aligned}$$

A.2.3 The numerical values of the control points of $H^{5,1}$

$\triangle^{5,1}$
Control points $h^{5,1}_{i,j,k}$ with $h^{5,1}_{i,j,k} = 0$: $h^{5,1}_{0,4,3}$, $h^{5,1}_{0,5,2}$, $h^{5,1}_{0,6,1}$, $h^{5,1}_{0,7,0}$, $h^{5,1}_{1,4,2}$, $h^{5,1}_{1,5,1}$, $h^{5,1}_{1,6,0}$, $h^{5,1}_{2,4,1}$, $h^{5,1}_{2,5,0}$, $h^{5,1}_{3,4,0}$
Control points $h^{5,1}_{i,j,k}$ with $h^{5,1}_{i,j,k} = 1$: $h^{5,1}_{4,0,3}$, $h^{5,1}_{4,1,2}$, $h^{5,1}_{4,2,1}$, $h^{5,1}_{4,3,0}$, $h^{5,1}_{5,0,2}$, $h^{5,1}_{5,1,1}$, $h^{5,1}_{5,2,0}$, $h^{5,1}_{6,0,1}$, $h^{5,1}_{6,1,0}$, $h^{5,1}_{7,0,0}$
Remaining control points $h^{5,1}_{i,j,k}$: $h^{5,1}_{0,0,7} = 0.2000000000$ $h^{5,1}_{0,1,6} = 0.2303117189$ $h^{5,1}_{0,2,5} = 0.2391872668$ $h^{5,1}_{0,3,4} = 0.2161176164$ $h^{5,1}_{1,0,6} = 0.2980907830$ $h^{5,1}_{1,1,5} = 0.3365903907$ $h^{5,1}_{1,2,4} = 0.3382083814$ $h^{5,1}_{1,3,3} = 0.2397844499$ $h^{5,1}_{2,0,5} = 0.4226781305$ $h^{5,1}_{2,1,4} = 0.4494178391$ $h^{5,1}_{2,2,3} = 0.4369312701$ $h^{5,1}_{2,3,2} = 0.2500000000$ $h^{5,1}_{3,0,4} = 0.5092096451$ $h^{5,1}_{3,1,3} = 0.6608722055$ $h^{5,1}_{3,2,2} = 0.7500000000$ $h^{5,1}_{3,3,1} = 0.5000000000$

$\triangle^{5,2}$

Control points $h^{5,2}_{i,j,k}$ with $h^{5,2}_{i,j,k} = 0$:

$h^{5,2}_{0,4,3}$, $h^{5,2}_{0,5,2}$, $h^{5,2}_{0,6,1}$, $h^{5,2}_{0,7,0}$, $h^{5,2}_{1,4,2}$, $h^{5,2}_{1,5,1}$, $h^{5,2}_{1,6,0}$, $h^{5,2}_{2,3,2}$, $h^{5,2}_{2,4,1}$, $h^{5,2}_{2,5,0}$, $h^{5,2}_{3,2,2}$, $h^{5,2}_{3,3,1}$, $h^{5,2}_{3,4,0}$, $h^{5,2}_{4,0,3}$, $h^{5,2}_{4,1,2}$, $h^{5,2}_{4,2,1}$, $h^{5,2}_{4,3,0}$, $h^{5,2}_{5,0,2}$, $h^{5,2}_{5,1,1}$, $h^{5,2}_{5,2,0}$, $h^{5,2}_{6,0,1}$, $h^{5,2}_{6,1,0}$, $h^{5,2}_{7,0,0}$

Remaining control points $h^{5,2}_{i,j,k}$:

$h^{5,2}_{0,0,7} = 0.2000000000$	$h^{5,2}_{0,1,6} = 0.1206428896$	$h^{5,2}_{0,2,5} = 0.0494736679$
$h^{5,2}_{0,3,4} = 0.0292775610$	$h^{5,2}_{1,0,6} = 0.2303117189$	$h^{5,2}_{1,1,5} = 0.1295184375$
$h^{5,2}_{1,2,4} = 0.0320427867$	$h^{5,2}_{1,3,3} = 0.0202302971$	$h^{5,2}_{2,0,5} = 0.2391872668$
$h^{5,2}_{2,1,4} = 0.1259083241$	$h^{5,2}_{2,2,3} = 0.0317364078$	$h^{5,2}_{3,0,4} = 0.2161176164$
$h^{5,2}_{3,1,3} = 0.0588827504$		

$\triangle^{5,3}$

Control points $h^{5,3}_{i,j,k}$ with $h^{5,3}_{i,j,k} = 0$:

$h^{5,3}_{0,4,3}$, $h^{5,3}_{0,5,2}$, $h^{5,3}_{0,6,1}$, $h^{5,3}_{0,7,0}$, $h^{5,3}_{1,4,2}$, $h^{5,3}_{1,5,1}$, $h^{5,3}_{1,6,0}$, $h^{5,3}_{2,3,2}$, $h^{5,3}_{2,4,1}$, $h^{5,3}_{2,5,0}$, $h^{5,3}_{3,2,2}$, $h^{5,3}_{3,3,1}$, $h^{5,3}_{3,4,0}$, $h^{5,3}_{4,0,3}$, $h^{5,3}_{4,1,2}$, $h^{5,3}_{4,2,1}$, $h^{5,3}_{4,3,0}$, $h^{5,3}_{5,0,2}$, $h^{5,3}_{5,1,1}$, $h^{5,3}_{5,2,0}$, $h^{5,3}_{6,0,1}$, $h^{5,3}_{6,1,0}$, $h^{5,3}_{7,0,0}$

Remaining control points $h^{5,3}_{i,j,k}$:

$h^{5,3}_{0,0,7} = 0.2000000000$	$h^{5,3}_{0,1,6} = 0.1206428896$	$h^{5,3}_{0,2,5} = 0.0494736679$
$h^{5,3}_{0,3,4} = 0.0292775610$	$h^{5,3}_{1,0,6} = 0.1206428896$	$h^{5,3}_{1,1,5} = 0.0677823437$
$h^{5,3}_{1,2,4} = 0.0544226687$	$h^{5,3}_{1,3,3} = 0.0202302971$	$h^{5,3}_{2,0,5} = 0.0494736679$
$h^{5,3}_{2,1,4} = 0.0544226687$	$h^{5,3}_{2,2,3} = 0.0626646441$	$h^{5,3}_{3,0,4} = 0.0292775610$
$h^{5,3}_{3,1,3} = 0.0202302971$		

Because of the reflectional symmetry of the blending functions of the N-surface-blends (H25) the control points of the Bézier-triangles $\triangle^{5,4}$ and $\triangle^{5,5}$ are given by

$$\begin{aligned} h^{5,4}_{i,j,k} &= h^{5,2}_{j,i,k} \\ h^{5,5}_{i,j,k} &= h^{5,1}_{j,i,k} \quad . \end{aligned}$$

A.2.4 The numerical values of the control points of $H^{6,1}$

$\triangle^{6,1}$

Control points $h^{6,1}_{i,j,k}$ with $h^{6,1}_{i,j,k} = 0$:
$h^{6,1}_{0,4,3}$, $h^{6,1}_{0,5,2}$, $h^{6,1}_{0,6,1}$, $h^{6,1}_{0,7,0}$, $h^{6,1}_{1,4,2}$, $h^{6,1}_{1,5,1}$, $h^{6,1}_{1,6,0}$, $h^{6,1}_{2,4,1}$, $h^{6,1}_{2,5,0}$, $h^{6,1}_{3,4,0}$

Control points $h^{6,1}_{i,j,k}$ with $h^{6,1}_{i,j,k} = 1$:
$h^{6,1}_{4,0,3}$, $h^{6,1}_{4,1,2}$, $h^{6,1}_{4,2,1}$, $h^{6,1}_{4,3,0}$, $h^{6,1}_{5,0,2}$, $h^{6,1}_{5,1,1}$, $h^{6,1}_{5,2,0}$, $h^{6,1}_{6,0,1}$, $h^{6,1}_{6,1,0}$, $h^{6,1}_{7,0,0}$

Remaining control points $h^{6,1}_{i,j,k}$:

$h^{6,1}_{0,0,7} = 0.1666666667$	$h^{6,1}_{0,1,6} = 0.2083818393$	$h^{6,1}_{0,2,5} = 0.2403598347$
$h^{6,1}_{0,3,4} = 0.2586222361$	$h^{6,1}_{1,0,6} = 0.2500970120$	$h^{6,1}_{1,1,5} = 0.3015493620$
$h^{6,1}_{1,2,4} = 0.3263334929$	$h^{6,1}_{1,3,3} = 0.2543111180$	$h^{6,1}_{2,0,5} = 0.3530017120$
$h^{6,1}_{2,1,4} = 0.3673550188$	$h^{6,1}_{2,2,3} = 0.4460695749$	$h^{6,1}_{2,3,2} = 0.2500000000$
$h^{6,1}_{3,0,4} = 0.3817083257$	$h^{6,1}_{3,1,3} = 0.6908541628$	$h^{6,1}_{3,2,2} = 0.7500000000$
$h^{6,1}_{3,3,1} = 0.5000000000$		

$\triangle^{6,2}$

Control points $h^{6,2}_{i,j,k}$ with $h^{6,2}_{i,j,k} = 0$:
$h^{6,2}_{0,4,3}$, $h^{6,2}_{0,5,2}$, $h^{6,2}_{0,6,1}$, $h^{6,2}_{0,7,0}$, $h^{6,2}_{1,4,2}$, $h^{6,2}_{1,5,1}$, $h^{6,2}_{1,6,0}$, $h^{6,2}_{2,3,2}$, $h^{6,2}_{2,4,1}$, $h^{6,2}_{2,5,0}$, $h^{6,2}_{3,2,2}$, $h^{6,2}_{3,3,1}$, $h^{6,2}_{3,4,0}$, $h^{6,2}_{4,0,3}$,
$h^{6,2}_{4,1,2}$, $h^{6,2}_{4,2,1}$, $h^{6,2}_{4,3,0}$, $h^{6,2}_{5,0,2}$, $h^{6,2}_{5,1,1}$, $h^{6,2}_{5,2,0}$, $h^{6,2}_{6,0,1}$, $h^{6,2}_{6,1,0}$, $h^{6,2}_{7,0,0}$

Remaining control points $h^{6,2}_{i,j,k}$:

$h^{6,2}_{0,0,7} = 0.1666666667$	$h^{6,2}_{0,1,6} = 0.1249514940$	$h^{6,2}_{0,2,5} = 0.0734991440$
$h^{6,2}_{0,3,4} = 0.0142880691$	$h^{6,2}_{1,0,6} = 0.2083818393$	$h^{6,2}_{1,1,5} = 0.1471923120$
$h^{6,2}_{1,2,4} = 0.0593130538$	$h^{6,2}_{1,3,3} = 0.0071440346$	$h^{6,2}_{2,0,5} = 0.2403598347$
$h^{6,2}_{2,1,4} = 0.1726485779$	$h^{6,2}_{2,2,3} = 0.0423846598$	$h^{6,2}_{3,0,4} = 0.2586222361$
$h^{6,2}_{3,1,3} = 0.0043111180$		

$\triangle^{6,3}$

Control points $h^{6,3}_{i,j,k}$ with $h^{6,3}_{i,j,k} = 0$:
$h^{6,3}_{0,4,3}$, $h^{6,3}_{0,5,2}$, $h^{6,3}_{0,6,1}$, $h^{6,3}_{0,7,0}$, $h^{6,3}_{1,4,2}$, $h^{6,3}_{1,5,1}$, $h^{6,3}_{1,6,0}$, $h^{6,3}_{2,3,2}$, $h^{6,3}_{2,4,1}$, $h^{6,3}_{2,5,0}$, $h^{6,3}_{3,2,2}$, $h^{6,3}_{3,3,1}$, $h^{6,3}_{3,4,0}$, $h^{6,3}_{4,0,3}$,
$h^{6,3}_{4,1,2}$, $h^{6,3}_{4,2,1}$, $h^{6,3}_{4,3,0}$, $h^{6,3}_{5,0,2}$, $h^{6,3}_{5,1,1}$, $h^{6,3}_{5,2,0}$, $h^{6,3}_{6,0,1}$, $h^{6,3}_{6,1,0}$, $h^{6,3}_{7,0,0}$

Remaining control points $h^{6,3}_{i,j,k}$:

$h^{6,3}_{0,0,7} = 0.1666666667$	$h^{6,3}_{0,1,6} = 0.0832363213$	$h^{6,3}_{0,2,5} = 0.0192803306$
$h^{6,3}_{0,3,4} = 0.0724710640$	$h^{6,3}_{1,0,6} = 0.1249514940$	$h^{6,3}_{1,1,5} = 0.0512583259$
$h^{6,3}_{1,2,4} = 0.0458756973$	$h^{6,3}_{1,3,3} = 0.0362355320$	$h^{6,3}_{2,0,5} = 0.0734991440$
$h^{6,3}_{2,1,4} = 0.0284741593$	$h^{6,3}_{2,2,3} = 0.0115457653$	$h^{6,3}_{3,0,4} = 0.0142880691$
$h^{6,3}_{3,1,3} = 0.0071440346$		

Because of the reflectional symmetry of the blending functions of the N-surface-blends (H25) the control points of the Bézier-triangles $\triangle^{6,4}$, $\triangle^{6,5}$ and $\triangle^{6,6}$ are given by

$$\begin{aligned} h^{6,4}_{i,j,k} &= h^{6,3}_{j,i,k} \\ h^{6,5}_{i,j,k} &= h^{6,2}_{j,i,k} \\ h^{6,6}_{i,j,k} &= h^{6,1}_{j,i,k} \quad . \end{aligned}$$

References

[BaBe87] R. H. Bartels, J. C. Beatty, B. A. Barsky. *An introduction to splines for use in computer graphics and geometric modeling.* Kaufmann, Los Altos, 1987.

[Boor87] C. de Boor. *A practical guide to splines.* Springer, New York, 1987.

[Diet98] U. Dietz. Fair surface reconstruction from point clouds. In M. Dæhlen, T. Lyche, and L. L. Schumaker, editors, *Mathematical Methods for Curves and Surfaces II*, pages 79–86. Vanderbilt University Press, 1998.

[Dier95] P. Dierckx. *Curve and surface fitting with splines.* Oxford Clarendon Press, 1995.

[EcHo96] M. Eck, H. Hoppe. *Automatic Reconstruction of B-Spline Surfaces of Arbitrary Topological Type.* ACM SIGGRAPH, 1996.

[FaSv96] R. A. M. T. Farouki, R. Sverrisson. *Approximation of rolling-ball blends for free-form parametric surfaces.* Computer-Aided Design, vol. 28, no. 11, 1996.

[Fari97] G. E. Farin. *Curves and surfaces for computer aided geometric design: a practical guide.* 1997.

[Floa98] M. S. Floater. *How to approximate scattered data by least squares.* Technical Report STF42 A98013, SINTEF, Oslo, 1998.

[GoSc88] M. von Golitschek, L. L. Schumaker. Data fitting by penalized least squares. In J. C. Mason, editor, *Algorithms for approximation II*, pages 210–227, Shrivenham, 1988.

[FlHo02] M. S. Floater, K. Hormann. Parameterization of triangulations and unorganized points. In A. Iske, E. Quak, and M. S. Floater, editors, *Tutorials on Multiresolution in Geometric Modelling*, Mathematics and Visualization, pages 287–316, Springer, 2002.

[HeKo96] T. Hermann, Z. Kovács, T. Várady. *Special Applications in Surface Fitting.* Theory and practice of geometric modeling, 1996.

[Horm00] K. Hormann. *Fitting Free Form Surfaces.* Principles of 3D Image Analysis and Synthesis, Kluwer Academic Publishers, 2000.

[Horm01] K. Hormann. *Theory and Applications of Parameterizing Triangulations.* PhD thesis, University of Erlangen-Nürnberg, 2001.

[HoLa93] J. Hoschek, D. Lasser. *Fundamentals of Computer Aided Geometric Design.* AK Peters, 1993.

[KoMa00] G. Kós, R. R. Martin, T. Várady. *Methods to recover constant radius rolling ball blends in reverse engineering.* Computer Aided Geometric Design, vol. 17, no. 2, 2000.

[LePe02] B. Lévy, S. Petitjean, N. Ray, J. Maillot. *Least Squares Conformal Maps for Automatic Texture Atlas Generation.* ACM Transactions on Graphics, vol. 21, no. 3, pages 362-371, 2002.

[Loop94] C. Loop. *A G^1 triangular spline surface of arbitrary topological type.* Computer Aided Geometric Design, vol. 11, 1994.

[Pete01] J. Peters. *C^2 Free-Form Surfaces of degree $(3, 5)$.* 2001.

[Schu81] L. L. Schumaker. *Spline Functions: Basic Theory.* John Wiley & Sons, New York, 1981.

[VaBe98] T. Várady, P. Benkö, G. Kós. *Reverse engineering regular objects: Simple segmentation and surface fitting procedures.* International Journal of Shape Modeling, vol. 4, no. 3 & 4, 1998.

[VaHo98] T. Várady, C. M. Hoffmann. *Vertex Blending: Problems and Solutions.* Mathematical Methods for Curves and Surfaces II, 1998.

[VaRo97] T. Várady, A. Rockwood. *Geometric construction for setback vertex blending.* Computer-Aided Design, vol. 29, no. 6, 1997.

[WaMe96] D. J. Walton, D. S. Meek. *A triangular G^1 patch from boundary curves.* Computer-Aided Design, vol. 28, no. 2, 1996.

[WeRe99] V. Weiß, G. Renner, T. Várady. *Reconstruction of swept free-form features from measured data points.* Proc. of 32nd CIRP International Seminar on Manufacturing Systems, 1999.